The Design and Testing of a Powered Exoskeleton to Reduce the Metabolic Cost of Walking in Individuals with Cerebral Palsy

By Michael O. Bair

A Thesis Submitted in Partial Fulfilment of the Requirements for the Degree of Master of Science in Mechanical Engineering

Northern Arizona University

May 2018

Approved:
Zachary Lerner, Ph.D. - Chair
John Tester, Ph.D.
Timothy Becker, Ph.D.
Kyle Winfree, Ph.D.

ABSTRACT

Mechanical Engineering Department

Master of Science in Mechanical Engineering

Application of Powered Exoskeletons to Reduce the Metabolic Cost of Walking in Individuals with Cerebral Palsy

By Michael O. Bair

ABSTRACT

Cerebral palsy (CP) is the most common form of motor impairment in children. Although CP is a non-progressive neurodevelopmental disorder, its secondary effects can lead to a decline in mobility over time. Eventually, individuals with CP may lose all ambulatory function. Interventions for CP, such as surgery and physical therapy, seek to delay the decline and improve mobility. Research into alternative interventions attempt to find improved outcomes over the traditional treatments. Robot-assistive devices are one such intervention that makes use of powered actuation, sensing, and control to help individuals with CP to retain and improve mobility.

The purpose of this research was to develop and test a robot-assistive device that reduces the metabolic cost of walking in children and young adults with CP. Our device consisted of an actuator-and-control module worn on the back, and two custom ankle-foot orthotics (AFOs). The control module contained brushless DC motors, electronics to control actuation, and a power supply. Plantarflexion, or "push-off", assistive torque was transferred from the motors to the orthotics using Bowden cables. 32-Bit ARM microcontrollers operated the system with inputs from force sensitive resistors (FSR) placed under the ball of each foot, and torque sensors aligned

with each ankle joint. Proportional gain control was used to control motor output torque. We implemented a two-state Finite State Machine (FSM) to control the timing of assistance.

We completed a pilot study with three participants with CP. We used indirect calorimetry to estimate metabolic cost. The study participants walked under three conditions: baseline, zero-torque, and powered assist. During the baseline condition, participants walked using their own shoes/AFOs and not our device. During the zero-torque condition, participants wore the device and the motors actively maintained a zero-torque reading at the ankle. During the assisted condition, participants wore the device while the motors gave plantarflexion assistance during late stance. Two participants had a decrease in metabolic cost between baseline and assisted conditions, an average of 16.5%. All participants showed an average reduction in the metabolic cost of walking of 40% between the zero-torque condition and the assisted condition, on average. Our youngest and lightest participant (5 years old, 16 kg) did not show a net decrease in metabolic cost between baseline and assisted walking, a result likely due to our device being a large percentage of their total mass, 12.5% as opposed to 7.5% and 4.4%.

We conclude that our device shows a strong potential for clinically-relevant applications. Further studies may show that robotic-assistance can improve mobility and quality of life in individuals with CP.

ACKNOWLEDGEMENTS

I would like to thank Dr. Zachary Lerner for guiding me through my research. His enthusiasm for my work and progress drove me to do more and become more. I am a better engineer and scholar because of his example.

I would also like to thank my colleagues for their invaluable help in this work. I thank Robert Libby for his work designing our custom PCBs. I thank Dr. Gian Maria Gasparri for his expertise in robotic controls. Together he and Mr. Libby provided the logic that made this work possible. I thank Hannah Rentschler, Joel Dewitt, and Jason Luque for their feedback on designs and assistance in fabricating the orthotics for our participants. Last, but not least, I thank Jason Luque, Jennifer Lawson, and Taryn Harvey for operating the Human Performance Lab and gathering the metabolic data.

Finally, I would like to thank Northern Arizona University for the great opportunity of being a student and researcher. This has been my greatest and most rewarding engineering experience.

DEDICATION

To my wife for her never ending support and encouragement. When I stumble, you steady me.

When I fall, you pick me up. When I succeed, you cheer with me.

CONTENTS

I. Research Overview 1

II. Cerebral Palsy 3

III. Biomechanics of the Gait cycle 5

IV. Mechanical Design 7

A. Design Considerations 8

B. Actuator Selection 11

C. Motor Selection 20

D. Effective Mass 22

E. Effective Mass Optimization 16

F. Torque Transmission 22

G. Material Selection 24

H. Component Design 24

I. Final Design 11

V. Electronics and Controls 35

A. PCB Design 35

B. Sensors and Controls 37

VI. Exoskeleton Analysis Method 40

A. Instrumentation 40

B. Pilot Study 41

VII. Results and Discussion 42

A. Metabolic Rate (Assisted vs. unassisted vs. typical) 42

B. Torque profile (Assisted vs. unassisted vs. typical) 44

C. Effective Mass metabolic prediction vs. measure metabolic rate 44

VIII. Conclusion 46

A. Limitations 46

B. Future Work 47

List of Tables

Table 1: Summary of main design considerations *9*

Table 2: Sample of Maxon 323218 motor datasheet. *21*

Table 3: Sample motor calculations *22*

Table 4: Comparison of effective mass configurations.....***Error! Bookmark not defined.***

Table 5: Comparison of the four considered materials *24*

Table 6: Comparison of estimated and measured metabolic increase .....***Error! Bookmark not defined.***

List of Figures

Figure 1: Basics of the Gait Cycle *5*

Figure 2: Major muscles used in the gait cycle *6*

Figure 3: A standard Bowden cable design *20*

Figure 4: The operation of Bowden cables *54*

Figure 5: A barrel adjuster *55*

Figure 6 The Turbomed FS3000 orthotic *26*

Figure 7: Insole bracket *26*

Figure 8: Ankle Pulley. *28*

Figure 9: Cable capture system *28*

Figure 10: FEA of the Ankle Pulley *29*

Figure 11: Initial motor pulley design ..... ***Error! Bookmark not defined.***

Figure 12: Final Motor Pulley design *30*

Figure 13: FEA of the motor pulley *31*

Figure 14: Motor Bracket *31*

Figure 15: FEA results for the Motor Bracket *32*

Figure 16: The Motor Cable Block *33*

Figure 17: FEA for the Motor Cable Block *34*

Figure 18: The Joint Cable Block *34*

Figure 19: FEA for the Joint Cable Block *35*

Figure 20: Custom PCB for the ankle Exoskeleton *36*

Figure 21: The Teensy 3.2 ..... *36*

Figure 22: Participant wearing the full system *41*

Figure 23: Measured metabolic rate *43*

Figure 24: Sample torque profiles *44*

I. Research Overview

Cerebral palsy (CP) is the most common form of motor impairment in children [1][2][3][4]. Typically, CP results from perinatal trauma of the brain or spine, or from congenital malformation of the brain [5][6]. The most commonly reported symptoms of CP include muscle weakness and spasticity, which usually results in decreased control, stability, movement speed, and movement efficiency [5][6]. Although the condition is non-progressive, children with CP typically suffer from a decline in mobility as they grow older [7][8][9].

CP has been shown to increase the energetic cost of walking by up to three times through reduced muscle function [10][11]. Walking requires careful coordination of muscle activation timing and magnitude [12][13]. In addition to propelling the body forward, muscles of the lower-extremity must maintain the body's balance and coordinate the motion of each limb. CP negatively impacts each of these requirements [5][6].

The primary goal of interventions for CP is to improve ambulatory ability. Standard interventions include physical therapy, surgery, and orthotic braces [14]. These are widely used, and have been shown to improve patient mobility. Research is being done to find other effective treatments; electrostimulation, whole body vibration, and botulin toxin injections have been found to have varying degrees of effectiveness [15][16][17][18].

A rapidly developing therapy is the use of robotic assistance. Robotic Assisted Gait Trainers (RAGTs) are typically large, expensive, stationary systems with powerful actuators that help impaired individuals follow a desired gait pattern [19][20][21][22]. This reduces the burden placed on physical therapists, who, traditionally, must move a patient's legs through the desired motion. This method improves both the repeatability of the motion and allows accurate

measurement of the patient's progress. Research has suggested a possible correlation between RAGTs and improvements in control, range of motion, and movement efficiency [20].

Another category of robot-assisted intervention is powered-assistive orthotics. While RAGTs may prove effective, they are limited to use in research clinics. RAGTs are typically large systems that are attached to a treadmill. Powered orthotics, or powered exoskeletons, are untethered devices that have potential to be used both in and out of the clinic [23][24]. They can be built for either rehabilitation, like RAGTs, or for augmentation. While rehabilitation seeks to restore lost mobility, augmentation seeks to replace lost mobility. Research has suggested that powered exoskeletons can improve mobility [25][26].

More research is needed to evaluate robot-assisted interventions for individuals with CP. Most devices that are designed for impaired individuals have not been tested on populations with CP. Stroke survivors are a common population where RAGTs and exoskeletons are currently being used. However, different disorders inhibit gait through different means and the effect of powered assistance on CP impaired gait has not yet been thoroughly explored.

Our long-term goal is to improve lives by increasing mobility and activity by sending these devices home with impaired individuals. This work bring us closer to that goal by designing and experimentally evaluating a battery-powered, assistive device specifically intended to improve walking economy. There were three major design requirements for this research. First, the device must be able to apply sufficient torque to assist gait. An appropriate amount of assistance for an individual is expected to reduce the net metabolic cost of walking. Second, the device must be battery powered to allow mobility. Our intent is to test a fully mobile device and not just an actuation system. To this end the system needs to last long enough for individuals to perform several walking trials while wearing the system. Third, the device must be affordable. A pair of

passive orthotic braces can cost up to $2000. Existing powered assistive device may be two orders of magnitude greater. We intend to develop a system that is within a single order of magnitude of passive orthosis. We expect that by reaching these goals we can positively impact the lives of individuals with CP by reducing the metabolic cost of walking and provide a testbed for future research.

II. Cerebral Palsy

Cerebral palsy (CP) is the most common form of motor impairment in children [1][2][3][4]. The cause of CP has been associated with many conditions and events including perinatal trauma and congenital malformation of the brain [5][6]. The most reported symptoms of CP include spasticity, reduced muscle strength, motor control, stability, general movement speed, and locomotor efficiency [5][6]. These symptoms often lead to a decreased range of motion, mobility, and thus quality of life.

CP is a non-progressive neurodevelopmental disorder that can affect muscle control and induce skeletal deformation [6]. Because CP affects the development of typical muscle control, it is common for individuals with CP to experience muscle tightness, called spasticity, and/or muscle weakness. This results in abnormal forces that can cause gradual bone deformation. Although CP is non-progressive, affected individuals usually experience a progressive decrease in mobility and quality of life [7][8][9].

Neuromuscular disorders like CP inhibit efficient walking. Level walking utilizes several major muscle groups working in careful synchronization to maintain balance, coordinate limb movement, and provide propulsion [12][13]. Both muscle spasticity and muscle weakness can restrict the range of motion of lower-extremity joints, reduce the ability to push forward, or

coordinate limb movement. Walking efficiency is typically significantly impaired [5][6]. While interventions to address gait deficits caused by CP are many and varied, they all seek to make walking easier, due to the greatly elevated energy cost of walking in this population [11]. Standard interventions include physical therapy, surgery, and orthotic braces [14]. It is hypothesized that walking ability may be improved by increasing muscle strength, control, and range of motion [14][27]. Extensive research is being done into additional interventions including electrostimulation, whole body vibration, and botulin toxin injections [15][16][17][18]. The long-term effectiveness of these methods are currently under investigation.

Robot-based interventions are recent developments in physical therapy. Robotic devices use a combination of sensors, actuators, and computer control to achieve desired outcomes. Robotic Assisted Gait Trainers (RAGTs) are typically large, highly instrumented, highly actuated systems developed for the rehabilitation of individuals with impaired gait [19][20][21][22]. RAGTs attach to the user's legs and guide them through desired gait patterns over an attached treadmill. Because they are stationary they can afford the higher mass of powerful and accurate components. The main advantages of RAGTs are that they can increase repeatability and accuracy of treatments.

Active orthoses are another category of robot-based intervention. Active orthoses, or powered exoskeletons, are similar to RAGTs in that they use sensing, control, and actuation to assist in mobility. However, they are much smaller and typically mobile. Two separate, but related goals may exist for an active exoskeleton. The first goal is rehabilitation where the intervention seeks to result in a lasting improvement in underlying function [21] [24]. The second is to assist the user, increasing mobility and reducing the required work of movement. In short, rehabilitation

seeks to restore mobility while assistance seeks to replace it. Active orthoses devices are relatively new and require more research to determine long-term efficacy [20][25][26].

Because the secondary effects of CP progress over time, early intervention is critical to prolonging walking ability. Young children with mild CP can often walk and run similar to typically developing children. However, due to secondary CP effects, such as bone deformation, mobility declines as they age. As bones twist the body tries to compensate via altered postures and movement patterns. These usually require more force to maintain, which leads to greater deformations. Eventually, many affected individuals become unable to walk. Early intervention to correct posture and encourage proper gait can delay these secondary effects.

III. Biomechanics of the Gait Cycle

Bipedal locomotion is an inherently unstable, yet efficient, mode of transportation. Walking is a complex process that requires whole-body balance, forward propulsion, and limb coordination [12][13]. The Gait Cycle, Figure 1, describes the phases of typical walking patterns.

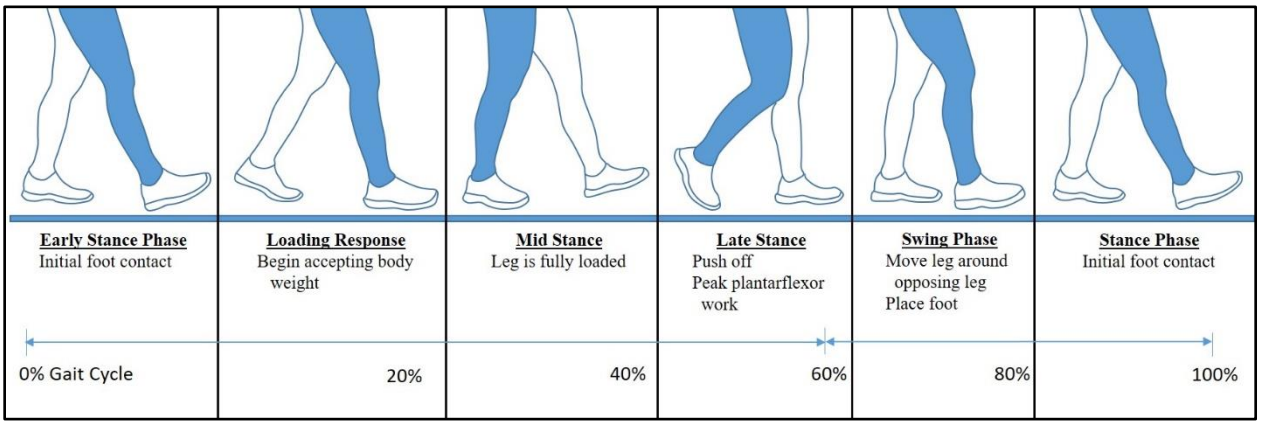

Figure 1: Basics of the Gait Cycle. The cycle begins with initial contact with the reference (blue) leg and ends when that leg returns to initial contact. The Cycle is divided into Stance phase and Swing phase.

The Gait Cycle describes a time-series sequence of events necessary for efficient walking. The Gait Cycle is divided up into two main phases, Stance and Swing. During the swing phase, the reference leg (shown in blue) is lifted off the ground, swings forward around the contralateral leg (shown in white), and is then placed on the ground. In the stance phase, the foot comes in contact with the ground, is loaded with the body weight, and then propels the body forward. During early stance phase, the contralateral leg is on the ground at the same time as the reference leg, a period called "double support". Following double support, the contralateral limb enters the swing phase, and the entire weight of the body is supported by the stance limb.

During unimpaired gait over 80% of all the work done during walking is done by the muscles that flex and extend the hip as well as the ankle plantarflexors and dorsiflexors [28]. The hip flexors move the mass of the leg during swing phase. The hip extensors and the ankle plantarflexors provide the majority of the forward propulsion [28][29]. Figure 2 highlights which muscles are primarily engaged at different points of the gait cycle.

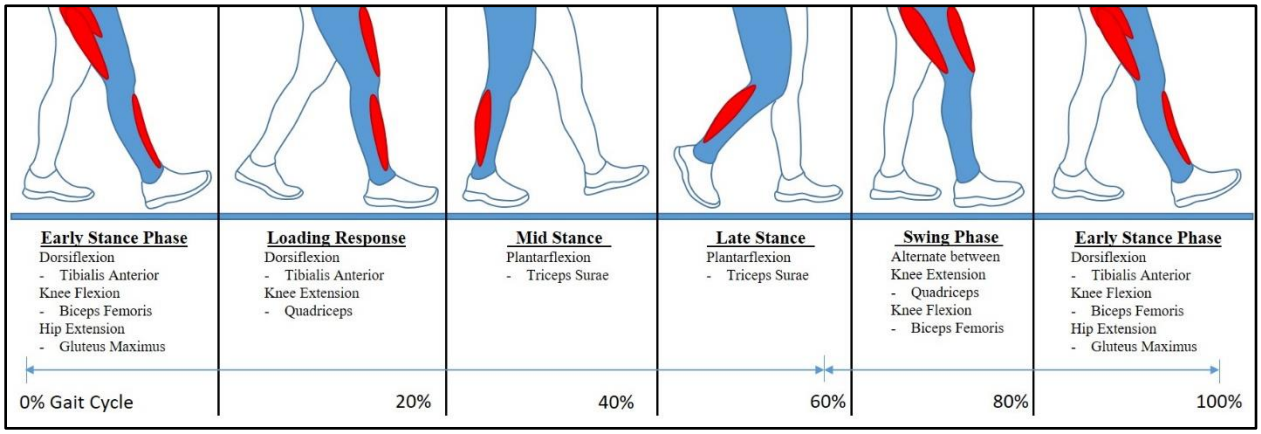

Figure 2: Major muscles used at different stages of the gait cycle. These muscles account for the majority of the work involved in walking. The ankle plantarflexor muscles and the hip flexors and extensors account for nearly all the work done during walking [28].

Neuromuscular pathologies, such as CP, negatively impact the gait cycle's repeatability and efficiency. Muscle weakness and spasticity prevent the muscles from applying desired forces and reduce range of motion. Skeletal deformities induced by the abnormal forces of spasticity and weakness can change where muscles apply forces, increasing the work necessary to walk.

CP affects individuals differently, making assistive device customization required to counteract specific pathologies. Assistive torques at the knee can improve knee extension and foot placement. Ankle plantarflexion torque can decrease the work required to walk and increase walking speed. Ankle dorsiflexion torque can improve stability by ensuring foot clearance during the swing phase.

IV. Mechanical Design

In Chapter IV we present the design of an assistive device that aims to reduce the metabolic cost of walking in children and young adults with CP. First, we review our main design and considerations. We then introduce our final design. The tools we developed and used are then introduced. Justification for our actuator, transmission, and material selections are given. Finally, the design of each component of our exoskeleton will be reviewed.

A. Design Overview

Our goal is to develop an ankle assistive device that can reduce the net metabolic rate of walking in children and young adults with CP. We hypothesized that powered ankle assistance will reduce the net metabolic cost of walking for individuals with CP by more than standard AFOs [30][31].

The ankle plantarflexor muscles provide between 40 and 50% of the work required in unimpaired gait [28][29]. Conversely, the muscles that cross the hip and knee provide approximately 40% and 20% of the work, respectively. This suggests that the ankle can receive the greatest benefit.

A single degree of freedom (DOF) system was used to reduce biological ankle work. Although the ankle is not a one-DOF joint, over 90% of the work done by the ankle is in dorsiflexion and plantarflexion [32]. We hypothesize that by providing only dorsiflexion and plantarflexion assistance we will reduce biological ankle work in individuals with CP.

B. Design Considerations

We identified torque output, mass, and range of motion as design criteria that correlate strongly with a reduction in the net metabolic rate of walking. Battery life and wireless communication criteria enable fully untethered operation. The torque output needed to be large enough to properly assist walking by augmenting existing muscle function [33] [34]. The mass added to the body needed to be low enough to not burden the user [35]. The range of motion needed to be sufficient enough to not impede the wearer [36]. Battery life needed to be long enough to allow several 5-minute walking trials. Finally, wireless communication was needed to allow recording, monitoring, and control system parameters.

Table 1 shows a summary of our main design goals.

Table 1: Summary of main design criteria. Values were selected based on data found in literature. Torque is mass normalized. Mass is given a percentage of body mass (BM).

Parameter	Goal
Torque	12 Nm
Mass	< 3 kg
Range of Motion	> 80°
Battery Life	> 30 minutes
Wireless	Bluetooth

Torque Increasing torque does not directly correlate to a decrease in metabolic rate. In 2017 a study of applied knee assistance in children with CP was conducted. In addition to reporting the kinetics and kinematics of the knee, they also reported the corresponding data for the ankle [33]. Their data shows that the peak ankle moment is approximately 1.0 Nm kg^{-1} with an average moment of 0.6 Nm kg^{-1}.

Our goal is to improve mobility and activity in individuals who use our device. Replacing total biological torque at the ankle will not increase the user's activity levels. To improve mobility while still engaging the user, we selected a maximum torque of 0.3 Nm kg^{-1}. Knowing that children in the upper range of our target demographic have a mass of 40 kg we therefore need a maximum torque of 12 Nm.

Mass Newton's Second Law states that the greater the mass, the greater the force required to accelerate it, $F = ma$. Moving a mass over a distance requires work; increasing the mass therefore increase the required work. Our muscles provide the force that moves the body by

converting metabolic work into mechanical work. Thus, an increase in mass requires more work done by the muscles, which raises the metabolic work done by the body.

Mass must be minimized to reduce the load on non-assisted joints. If the ankle is heavily loaded but equally assisted such that no extra work from the ankle plantarflexors and dorsiflexors is required there will still be a net increase in metabolic cost of walking. This is because the hip and knee, which are not assisted, must still move the extra mass at the ankle. To see positive results our design must have a low mass.

A 2004 study showed that the relationship between increasing mass to increasing metabolic rate of walking is non-linear [35]. It was shown that a 10% increase in mass would result in an estimated 17% increase in metabolic rate while a 50% increase in mass would result in a 100% increase in metabolic rate. We selected 10% body mass as our target goal. We believe that this is an acceptable increase. The smallest mass in our target demographic is 18 kg, resulting in a 1.8 kg device.

Range of Motion The range of motion of the exoskeleton must be sufficient enough that any user will not be restricted. Literature shows that the typical total range of motion of the ankle is between 65 and 75° [36]. We therefore set the target range of motion of the exoskeleton to be greater than 80° to ensure that our system does not impede any type of ankle movement.

Battery Life Functional testing of our system requires that the user be able to walk for a minimum of five minutes. It is typical for a person's metabolic rate to take three or four minutes to reach steady-state. A five-minute walking trial would allow for a minimum of one minute of metabolic data to be collected. By having a battery life greater than 30 minutes the user can perform multiple walking trials.

Wireless Communication Wireless communication would enable the user to move completely untethered while still allowing us to record, monitor, and control system parameters. However, wireless communication is an additional drain on the battery. To minimize this effect we selected Bluetooth communication as it is a low-power communication protocol.

C. Final Design

We developed three iterations of the exoskeleton before the design was finalized. The first design focused on functionality to prove the concept was reasonable. The second design focused on weight reduction and mass optimization. The third, and final, design further reduced weight, friction, and profile while seeking to improve user comfort and system stability. The final design, shown in Figure 3-Figure 6, weighed 2.0 kg. A summary of component masses and costs can be seen in Table 2.

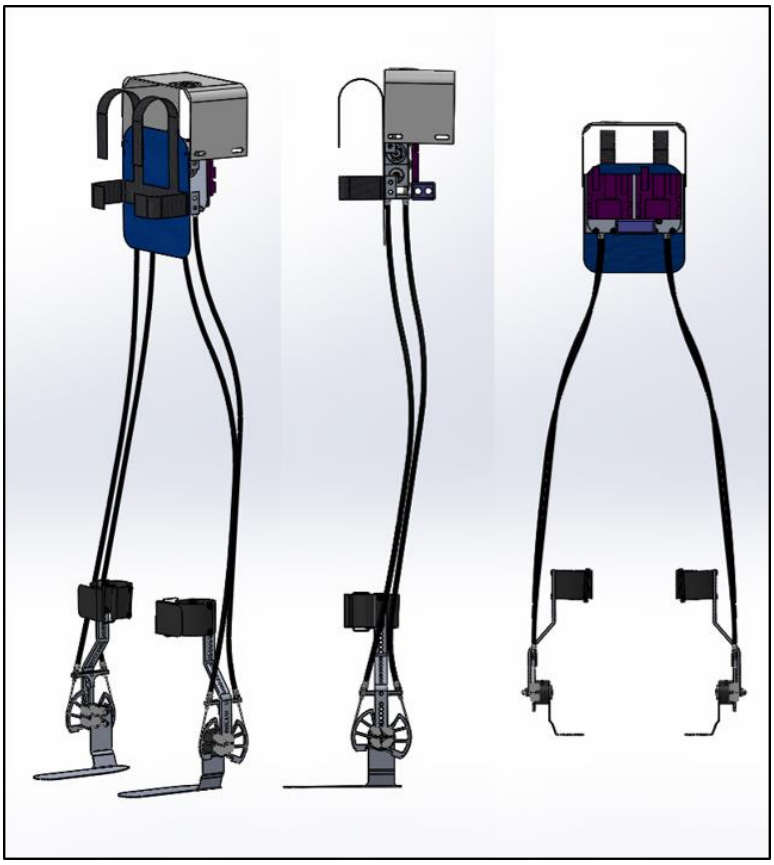

Figure 3: Model of the final exoskeleton. The design consists of a back-mounted control module, a Bowden cable transmission, and lightweight orthotics. The total mass of the system is 2.0 kg.

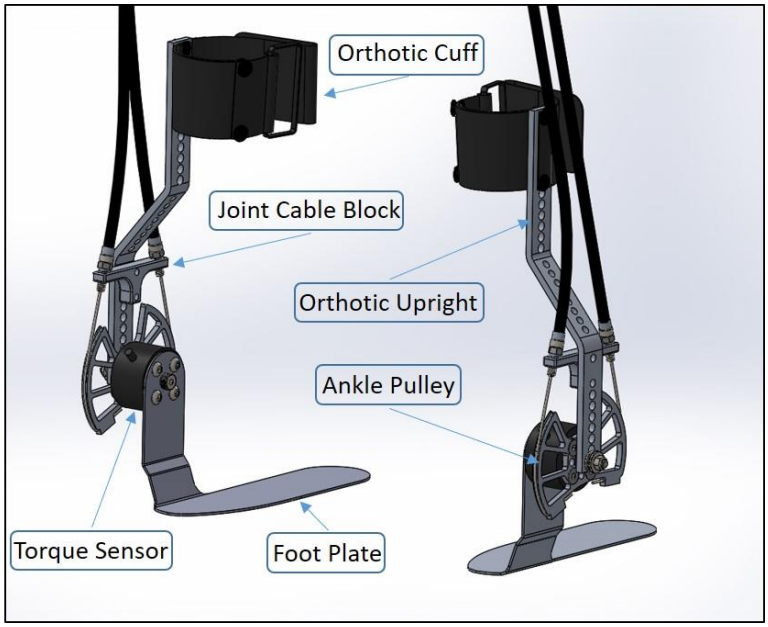

Figure 4: Model of the ankle orthotics. Torque is transmitted from the Bowden cable transmission system to the ankle pulley. Torque is measured by the torque sensor and transferred to the foot plate.

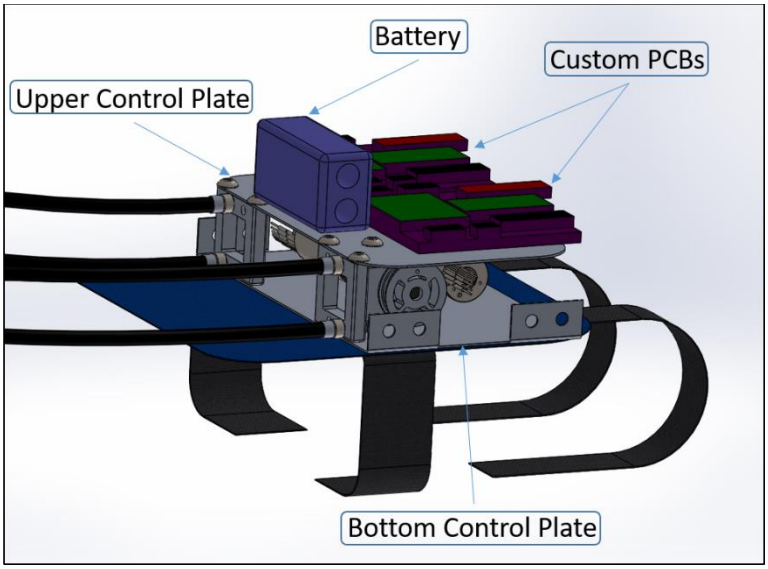

Figure 5: Model of the Upper Control Plate and components. The Upper Control Plate is the mounting point for the battery and our control electronics.

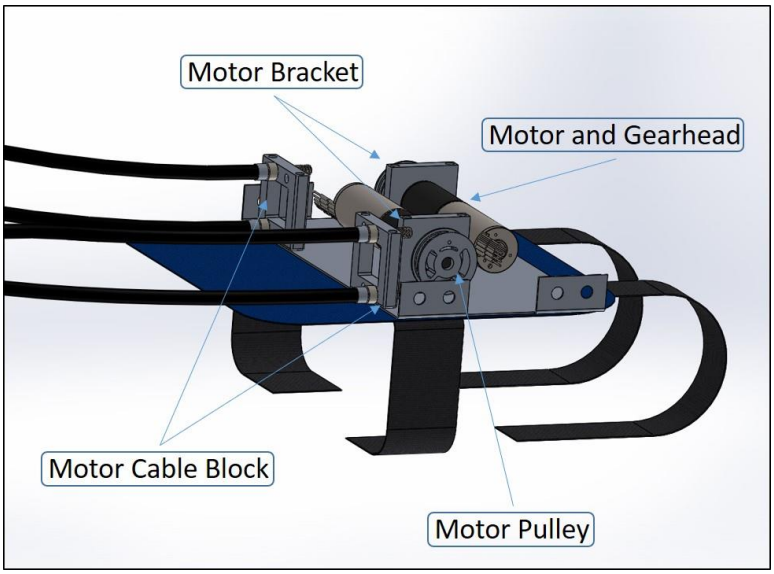

Figure 6: Model of the Lower Control Plate and components. The Lower Control Plate is the mounting point for our motors and is the proximal end of our transmission system.

Table 2: Summary of component masses and costs. The motor and gearbox assembly, the backpack, and the aluminum used in the control module (Mounting Assembly) are the most massive components. The torque sensors and motors are the most expensive.

Part	Mass	Units	Quantity	Total	Cost	Total
Motors/gearhead	200	g	2	400	$ 618.15	$ 1,236.30
Backpack	200	g	1	200	$ 29.99	$ 29.99
Mounting Assembly	200	g	1	200	$ 14.00	$ 14.00
Battery	137	g	1	137	$ 34.70	$ 34.70
Misc	100		1	100	$ 40.00	$ 40.00
Torque Sensor	65.6	g	2	131.2	$ 647.00	$ 1,294.00
Upright	46	g	2	92	$ 3.87	$ 7.74
Foot Plate	45	g	2	90	$ 14.00	$ 28.00
Cuffs	40	g	2	80	$ 4.00	$ 8.00
Motor Drivers	30		2	60	$ 157.15	$ 314.30
Ankle Pulley	20.2	g	2	40.4	$ 228.88	$ 457.76
Joint Cable Block	15.3	g	2	30.6	$ 117.25	$ 234.50
Teensy 3.2	15		2	30	$ 24.23	$ 48.46
PCBs	15	g	2	30	$ 20.00	$ 40.00
Motor Cable Block	14.5	g	2	29	$ 133.49	$ 266.98
Motor Bracket	13.3	g	2	26.6	$ 110.63	$ 221.26
Motor Pulley	10.5	g	2	21	$ 196.89	$ 393.78
Cables	2	g/cm	200	400	$ 0.10	$ 20.00
			Grand Total	2097.8 g		$ 4,689.77

D. Effective Mass

Minimizing mass was one of our most critical requirement. It is intuitive to understand that a heavy system will impede the user. However, additional consideration must be made for the arrangement of the mass of the system. This section will analyze considerations of mass placement with regard to its effect on the energetics and biomechanics of walking.

The lower a mass is placed on the leg the greater the impact on gait biomechanics. We know that an increase in mass requires an increase in force to move it. We also know that the further away a mass is from the pivot point the greater the force or torque required to rotate it. In 2007, data relating mass location and metabolic rate were presented [37]. To better apply their work to lower-limb exoskeleton design, we have used their data to develop a simple mathematical relationship between lower-extremity mass locations and a metabolically-equivalent mass located at the waist. We introduce the effective mass equation in (1):

$$M_E = W + 1.667T + 1.689S + 4.444F \quad (1)$$

where M_E is the effective mass and W, T, S, and F are masses added at the waist, thigh, shank, and foot segments of the leg, respectively. Each mass is multiplied by a coefficient to equate it to a waist-mounted mass having the equivalent metabolic effect. Note that thigh (T) and shank (S) have nearly the same coefficient, which highlights the complexities of energy transfer throughout the lower extremity during walking.

Mass added to the foot increase the net metabolic rate 4.44 times more than the same amount of mass added to the waist. This shows that our design will likely benefit from moving all possible components to the waist.

The effective mass equation (1) can be used to objectively compare how the added mass of different designs and configurations would affect a user's metabolic cost. Because the human

body is a very complex system, a direct comparison of total mass is ineffective. The effective mass equation assumes that all masses are placed on the Center of Gravity (COG) of their respective limb segments. For our analysis of different ankle exoskeleton designs (section IV.E), we also assumed that components were placed on the nearest COG. This estimation will introduce error into our Effective Mass calculation but it will still provide valuable insight into our design.

Using the Effective Mass equation, we can estimate the net increase of metabolic rate from masses added to the leg. In [35] the relationship between mass added at the waist and walking metabolic rate is given as:

$$\dot{q}_{net} = 4.60m - 6.23m + 4.28 \quad (2)$$

where $\dot{q}_{net}$ is the net metabolic rate and m is the combined body weight and mass as a fraction of body weight. Standard practice in literature is to report changes in metabolic rates as a percentage of the base walking metabolic rate so we divide (2) by the base walking metabolic rate, q_{base}.

$$\dot{q}_{add} = \frac{4.60m - 6.23m + 4.28}{q_{base}} \; x\; 100 \quad (3)$$

where $\dot{q}_{add}$ is the percent increase in net metabolic rate during walking.

E. Effective Mass Optimization

The Effective Mass equation previously introduced was used to evaluate designs based on component locations. Several options exist for how the powered ankle exoskeleton will add mass to the body. While some components must be placed at the ankle, such as sensors and orthotics,

other components can be placed either at the joint or elsewhere on the body, such as the motors and power supply. Calculating the effective mass of different configurations of components can be used to estimate an optimal design (i.e. the design that minimizes the increase in metabolic cost when the exoskeleton is worn).

We determined that the lowest effective mass exists when the actuators, power supply, and controllers are placed above the waist. We considered four possible configurations and calculated their effective increase in metabolic cost. For each configuration all non-orthosis components, shown in Figure 5 and Figure 6, were placed at either the foot, shank, thigh, or above the waist. The ankle orthotics, Figure 4, remained at the foot and shank. Table 2 shows the mass of each component used in model. **Error! Reference source not found.** contains the calculated effective m asses for each configuration. As can be seen, the waist, or our backpack design in Figure 3, has the lowest effective mass.

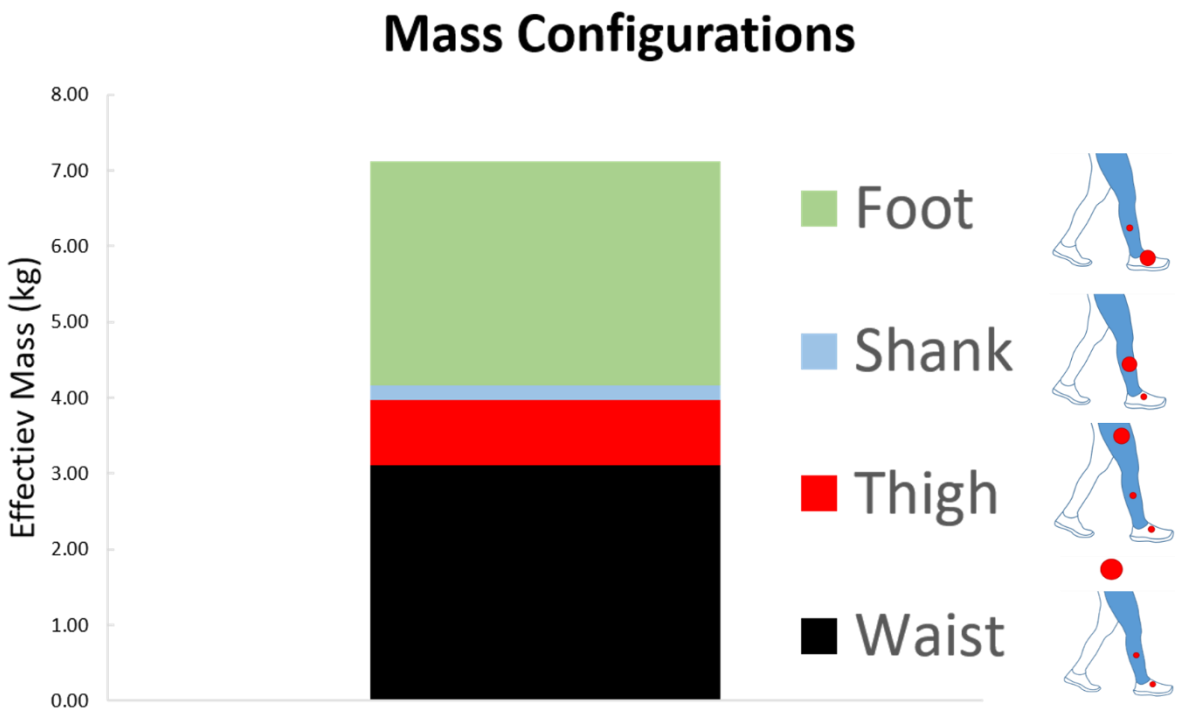

Figure 7: Comparison of effective mass configurations and estimated net metabolic increase for a 2kg device placed on a 20kg individual. The waist configuration has the lowest effective mass. The size of placement of the red circles correlates to the distribution of mass in each configuration.

F. Actuator Selection

The selection of actuator(s) largely determines the complexity, size, shape, and limitations of the system. For this assistive device to be effective, the actuator needed to be lightweight, reliable, and responsive. These criteria were used when considering hydraulic, pneumatic, and electric actuation and ultimately led to the selection of high-performance brushless DC motors.

Hydraulic actuators are too massive to be feasible for a light, untethered device. Hydraulic-based actuators are fast, powerful, and easily controlled. However, they also require a pump, fluid reservoir, and pressure regulators. It has been used in systems at Sarcos Robotics [38] and Ekso Bionics[39] but these are typically very heavy devices. While viable for larger systems that actuate all joints in the leg the minimum mass required would far exceed our design goals.

Pneumatic actuators have many similar advantages and drawbacks to hydraulic actuators. Pneumatic systems are powerful compared to human muscles and can react quickly when required. Furthermore, because gas is compressible there is a natural damping effect which would reduce actuator vibrations and may increase user comfort. Unfortunately, this type of system also requires a pressure supply and regulators and it is difficult to control accurately. In [40] the final mass of just the actuation system was 1.9 kg per leg with a 1.1 kg power supply and regulator at the waist. Operating two legs would result in a mass of 6.2 kg, far greater than our stated goal.

DC motors have important advantages over other actuators. DC motors have high power-to-weight ratios, making them ideal for lightweight systems. They can be extremely efficient with some motor efficiencies exceeding 90%. DC motors directly convert electrical energy into mechanical energy, ideal for battery-powered devices. Finally, high accuracy control of speed, torque, and position are possible with the addition of a few sensors.

DC motors also come with distinct challenges. The most efficient DC motors, brushless DC (BLDC), require complicated software controls and electronics to operate due to their nonlinear nature. The controls to drive the motor can either be purchased in a dedicated controller chip or the program and electronics must be developed. Another disadvantage is that motor speed and torque are inversely related. A motor cannot be driven at both peak speed and peak torque. Finally, DC motors are typically low torque devices. Even at very low speeds the output torque is insufficient for this application. Large gear reductions are required to reach our required torque magnitude.

Despite their disadvantages, DC motors were selected due to their critical advantages over other actuators. The high power-to-weight ratios and high efficient electrical-to-mechanical power conversion were the main reasons for our decision.

G. Motor Selection

Maxon Motors, Inc., develops very high quality, compact motor and gear head solutions in a wide range of sizes and power. Our primary motor selection criterion was to find a motor/gearhead combination that would efficiently deliver between 8-12 Nm of torque, sufficient for a 20-30 kg individual according to our calculations in section IV.B. Our secondary criterion was to find the lightest motor available.

The EC-4pole motor category, Maxon's highest quality line, had the best power-to-weight ratios. All the motors in this category could be paired with a gearhead to deliver acceptable torques. The motors were first sorted by lowest power and then by lowest mass. Motor power requirements were calculated at the maximum efficiency point for each motor. Table 3 shows a summary of the eight different motors considered. The EC-4pole22 brushless motors, models 323217 and 323218, top the list as the two best considerations. 323218 was ultimately selected for the slightly lower gear reduction required.

Table 3: Motor selection table. Primary selection criteria were minimal mass and minimal power consumption at max efficiency. Motors 323217 and 323218 were selected as the two best candidates, shown in red. 323218 was used in the final design for the slightly lower gear reduction (GR) ratio required.

Model #	Mass (g)	Power (W)	Efficiency	Motor Output (mNm)	Required GR
323217 (18V)	120	54.670	0.879	34	294
323218	120	57.989	0.883	36	278
311535 (18V)	170	79.765	0.886	48	208
311536	170	85.437	0.890	51	196
309756	210	147.470	0.856	85	118
309755 (18V)	210	150.993	0.856	87	115
468312	300	88.763	0.911	51	196
305013	300	279.968	0.887	169	59

We chose the GP22HP planetary gearhead, model 370782 to be paired with our motor. This planetary gear has an 89:1 gear reduction. Because we approximately require a 278:1 gear reduction we would need an additional 3:1 gearing between the output shaft and the ankle. We achieved this using a simple pulley system.

Motor selection was chosen using standard DC motor equations. Table 4 contains the relevant data to make these calculations and a sample of the calculations are in Table 5.

Table 4: Sample of information taken from the datasheet for the Maxon 323218 motor.

Variable	Line Item	Symbol	Value	Units
No-load speed	Line 2	n_0	16300	Rpm
No-load current	Line 3	M_0	164	mA
Stall current	Line 7	M_H	639	mNm
Torque constant	Line 12	k_M	14	mNm/A

For a given torque, the loaded speed is governed by Equation (4):

$$n = n_0 + \frac{M\, n_0}{M_H} \tag{4}$$

where n is the motor speed, n_0 is the no-load speed, M is motor torque, and M_H is the stall torque.

For a given torque, the current draw is governed by:

$$I = \frac{M}{k_M} + M_0 \tag{5}$$

where I is the current draw, M is the motor torque, k_m is the torque constant, M_0 is the stall torque.

For a given torque, the mechanical power is governed by:

$$P_M = Mn\frac{2\pi}{1000} \quad (6)$$

Where P_m is the mechanical power, M is the motor torque, and n is the motor speed.

Finally, the efficiency, calculated as power out (mechanical) over power in (electrical) is:

$$\eta = \frac{P_M}{P_{el}} \quad (7)$$

where η is the motor efficiency, P_M is the mechanical power, and P_{el} is the electrical power.

Table 5: Sample calculations to determine torque at max efficiency for motor model number 323218. The maximum efficiency point is highlighted in red.

Torque (mNm)	Speed (rpm)	Current (A)	Power (W)	Efficiency (%)
33	15458.5	2.52	53.42	88.29
34	15433	2.59	54.95	88.31
35	15407.5	2.66	56.47	88.32
36	15382	2.74	57.99	88.33
37	15356.5	2.81	59.50	88.33
38	15331	2.884	61.01	88.32
39	15305.5	2.95	62.51	88.30

As can be seen in Table 5, maximum efficiency for the 323218 motor occurs between 36 and 37 mNm of torque. Paired with our 89:1 gearhead and a 3:1 pulley system, for a total of 267:1 gear reduction, the output torque is 9.61 Nm. This is close to our desired torque output.

H. Torque Transmission

Because we have chosen to use BLDC motors placed above the waist we needed a long transmission system. Our design challenge was to find a transmission that was able to conform to human gait patterns. During walking the straight-line distance between the foot and the waist changes. Chain and belt driven transmissions require fixed points that are connected in a straight line and do not vary in length. Chain and belt transmissions are not easily compatible with our

design. These solutions would require several intermediate pulleys or idlers spaced along the leg, increasing mass and complexity.

An alternative solution is a Bowden cable transmission, which is comprised of an inner wire and an outer housing. Bowden cables are simple, lightweight, and flexible. Because of its flexibility it is able to conform to the movements of the wearer. Its mass is also extremely low, reducing the impact of the transmission system on natural biomechanics. The mass of the Bowden cable transmission is less than 2 g/cm.

A Bowden cable has two main components, the inner wire and the outer housing, shown in Figure 8. The wire is the actuator and the housing is stationary. The wire may be a simple uncoated cable or it can be coated with PTFE to reduce friction. The housing has three components, an inner plastic liner to lower friction, a tightly wound metal wire structure, and a plastic exterior, as shown in Figure 8.

Figure 8: A standard Bowden cable design. From outer to inner: plastic sheath, metal coil, inner plastic tube, and actuating inner cable. The housing, metal coil, and plastic tube comprise the stationary housing.

Bowden cables were chosen as our transmission system for simplicity and flexibility. An overview of the operation of Bowden cables can be found in Appendix A.

I. Material Selection

Exoskeletons generally require at least two different materials, one to handle the mechanical loads and one to interface with the body. This is analogous to the hard and soft tissues of the body. For the hard tissue, the bones, we selected Aluminum 6061-T6 because of its strength, low weight, and low cost.Table 6 shows comparisons of the four materials considered. For the soft tissue we chose to use Kydex thermoplastic because it can easily conform to the body when heated but become sufficiently stiff when cooled. However, for the foot plate we chose to use Aluminum. Although the foot plate interfaces with the foot we needed the strength of aluminum because of the loads that the exoskeleton would apply to the foot. Sufficient padding was used between plate and foot to allow for a more comfortable fit.

Table 6: Comparison of the four considered materials. While Aluminum 6061-T6 has the lowest strength it is the easiest to manufacture and is much cheaper than other materials. Prices are taken from mcmaster.com and are for 8"x8"x0.25"sheet for all materials except for titanium which is 6"x6"x0.125". Note that the price of titanium is several times greater than all other metals listed.

Material	Yield Strength (MPa)	Mass Density (kg/m^3)	Manufacturability	Cost ($)
Aluminum 6061-T6	275	2700	1	16.88
Steel Low Carbon	413	7750	2	30.63
Steel 4140	415	7850	2	43.72
Titanium Grade 5	1100	4430	3	159.25

J. Component Design

The design of all custom components will now be presented with a breakdown of features and a summary of structural integrity performed using Finite Element Analysis.

Foot Plate Applying torque around the ankle is a critical feature of the exoskeleton. It requires forces to be applied to the foot and the shank. Three different methods of applying loads to the foot were considered. The methods were: a plate in the shoe, a plate under the shoe, and a structure encasing the shoe.

A plate under the shoe would inhibit natural gait. Typical gait involves a smooth rolling transition from heel to toe. A rigid plate under the shoe would prevent this rolling action. The foot would essentially start with initial heel contact but then transition to flat-footed mid-stance prematurely. It was anticipated that this would be uncomfortable and hurt gait kinematics.

Another method considered was attaching a semi-rigid structure to the outside of the shoe. This idea was inspired by an orthosis designed by TurboMed to treat drop foot, the FS3000. Shown in Figure 9, the FS3000 is essentially a single structure wrapped across the top and back of the foot and it then attaches to the shank. The orthosis passively promotes dorsiflexion through elastic strain. This structure has a sufficiently strong connection to the shoe. During normal walking and running it does not disconnect or slip. The primary reason this design was not pursued at this time was due to our concern that either the connection or the material would not be able to withstand our applied loads. Furthermore, we would either need to purchase and modify a KS3000 or manufacture something similar. The design would likely be difficult to manufacture, and modification may also be difficult. Future research may involve exploring this concept.

Figure 9 The Turbomed FS3000. A unique design for providing dorsiflexion assistance.

We chose to use a simple rigid shoe insert. This design does not affect how the sole of the shoe interacts with the ground, unlike a plate under the shoe. This allows for a more regular heel-to-toe walk. Insole padding between plate and foot also helps lessen changes to walking patterns. The insert is also simple enough to be fabricated with common tools. Figure 10 shows the insole design. Instructions for manufacturing can be found in Appendix B.

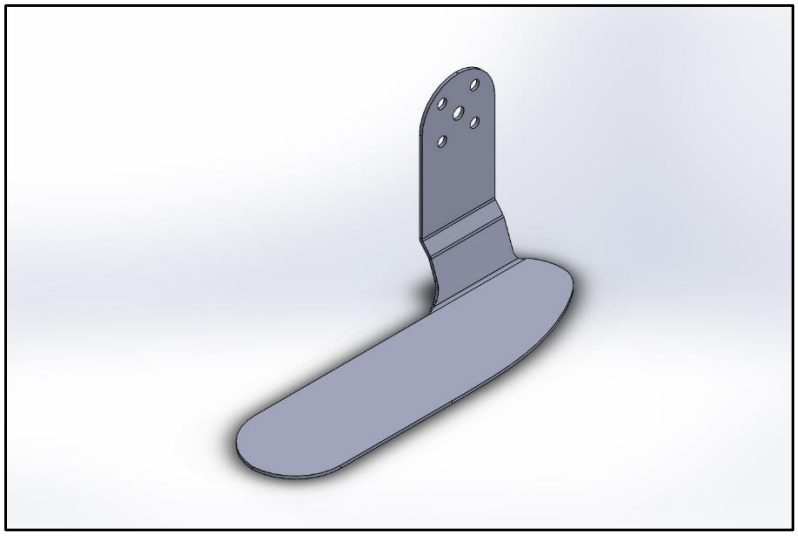

Figure 10: Insole bracket. The four bolt pattern attaches to the torque sensor. The central hole is for the shoulder bolt that the ankle assembly attaches to.

A concern when designing the insole plate was that it would be uncomfortable under the foot and at the ankle. By placing the plate under the padded insole of the shoe, the change in stiffness and contour caused by the foot plate is almost negligible to the user. The lateral, upright portion of the plate is located far enough away from the user's ankle that interaction is rare. A small piece of foam over the bolts ensures that the user is not hurt by bolt heads.

Ankle Pulley Torque transfer from the motor to the ankle required a way of attaching the Bowden cables such a 3:1 gear reduction is maintained across the pulley's entire range of motion. DC motors and body joints are rotational systems, however the Bowden cable transmission is translational. To convert from rotation, to translation, and back to rotation, we developed a pulley for the motor and another for the ankle.

The pulley was designed with minimal mass and a sufficient range of motion. Unlike traditional pulleys, our design does not need to spin freely. Our pulley only needed to rotate 50 degrees in plantarflexion and 30 degrees in dorsiflexion. Because of this we were able to remove large sections of the pulley to reduce the mass as shown in Figure 11. Range of motion was further optimized by offsetting the torque sensor bolt hole pattern. The pulley is symmetric except for the bolt holes, which have been rotated 10 degrees. This changes the range of motion from 40 degrees in both plantarflexion and dorsiflexion to 50 degrees plantar flexion and 30 degrees dorsiflexion.

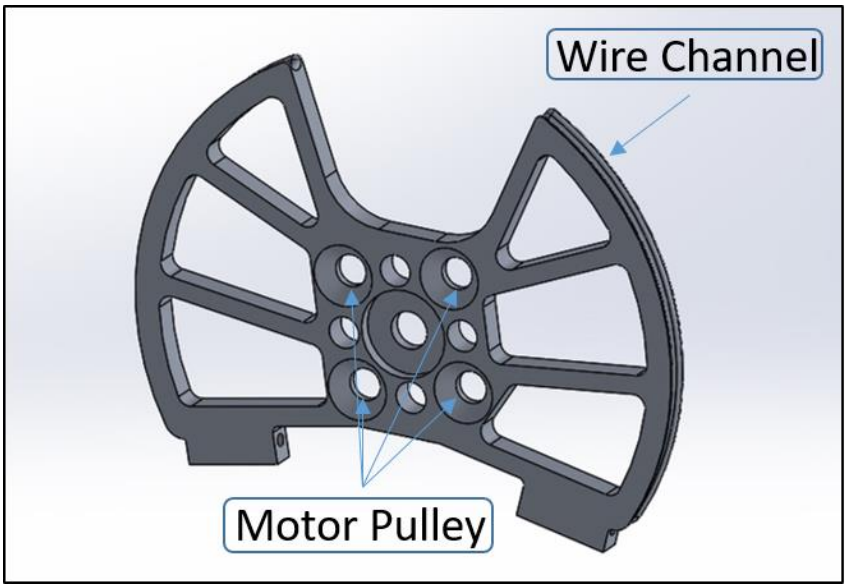

Figure 11: Model of the Ankle Pulley. Large sections of the pulley were removed to minimize mass. Enough of the pulley circumference remains to allow for the full range of motion of the ankle.

Because the ankle pulley was the distal end of the transmission, the pulley has a redundant capture system for the Bowden cable, Figure 12. This system uses two set screws to crimp the cable in place. This method has been tested up to 12 Nm of torque without failure.

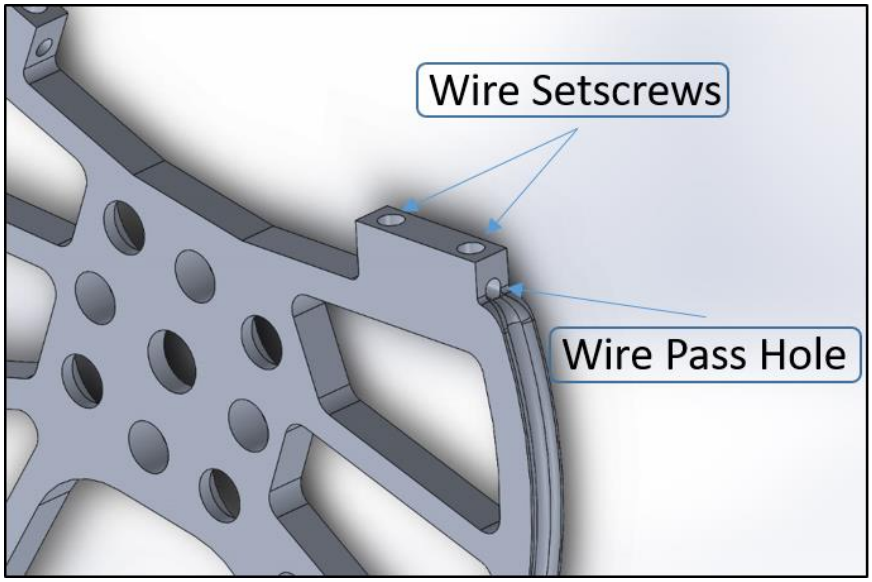

Figure 12: Cable capture system uses two set screws to crimp the Bowden cable in place.

In IV.G we showed that a 3:1 gear reduction needed to exist between the motor assembly and the ankle. The ankle pulley is the distal end of that reduction and is three times the diameter of the proximal pulley that is attached to the motor shaft.

The minimum mass of the ankle pulley was mostly restricted by Bowden cable wire diameter. A channel along the circumference of the pulley was included to accommodate the Bowden cable's inner wire. The wire has a diameter of 1.6mm so the channel is 2.0mm to prevent friction between wall and wire. A wall thickness of 1 mm was placed on either side of the cable to ensure that the actuating loads would not deform the channel or damage the part. This resulted in a 4mm thick pulley with a mass of 20.2g.

This prototype was designed to be as simple and as manufacturable as possible without hindering performance. This pulley has the fewest features we could design while still meeting our performance goals. The thickness is uniform, the weight-saving holes are few and large, and geometries were as simple as possible. However, some complicated features do still exist, such as the wire channel and the capture system. The ankle pulley had a factor of safety of 1.8 under a load of 270N, or the load required for 12 Nm of torque.

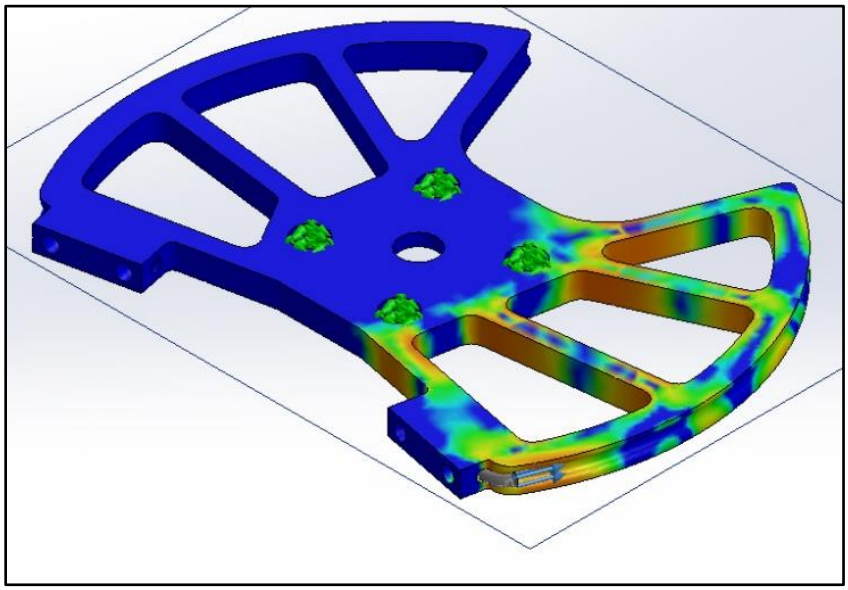

Figure 13: FEA of the Ankle Pulley. The factor of safety is 1.8.

Motor Pulley Torque transmission from the motor to the ankle required a method for rigidly attaching the Bowden cable while providing sufficient range of motion. Because the motor pulley is part of the Bowden cable transmission system the inner wire must be firmly affixed to the pulley while allowing a total of 240 degrees of rotation.

Our final design had a hole drilled through the inner wall of the pulley with a set screw hole intercepting it from the side, shown in Figure 14. The wire was wound 180 degrees around the pulley, passed through the hole, and then wound another 180 degrees. The set screw crimped the wire in place. We have achieved torques of 12 Nm without slippage and have nearly 270 degrees range of motion, which exceeds our minimum requirement.

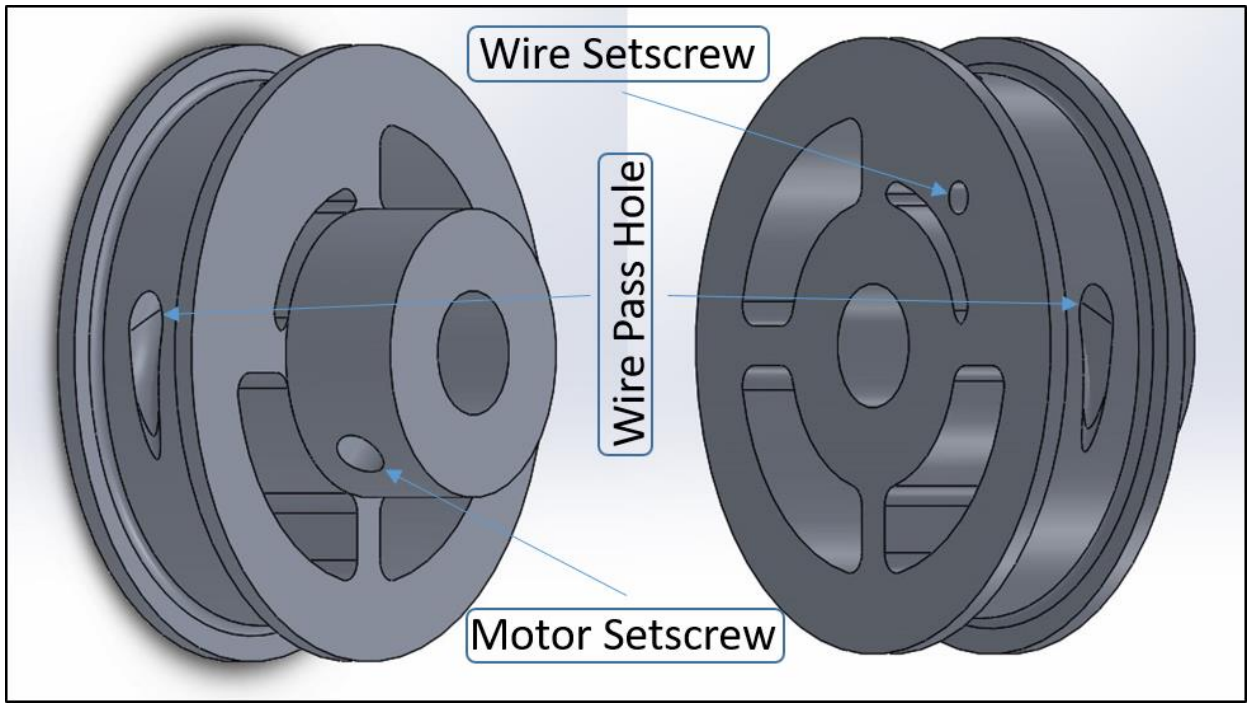

Figure 14: The Motor Pulley. A set screw on the center shaft attaches to the motor shaft. The hole in the cable trough allows the cable to pass through be crimped by the set screw in the wall.

Other features include weight saving holes, wide channels, and a set screw to attach the pulley to the motor output shaft. The channel for the inner wire needed to exceed 3x the wire diameter to limit friction from the wire interacting with itself. Torque transfer from the motor to the pulley used a single set screw. The factor of safety of this design, Figure 15, was 6.4 with a mass of 10.5 g.

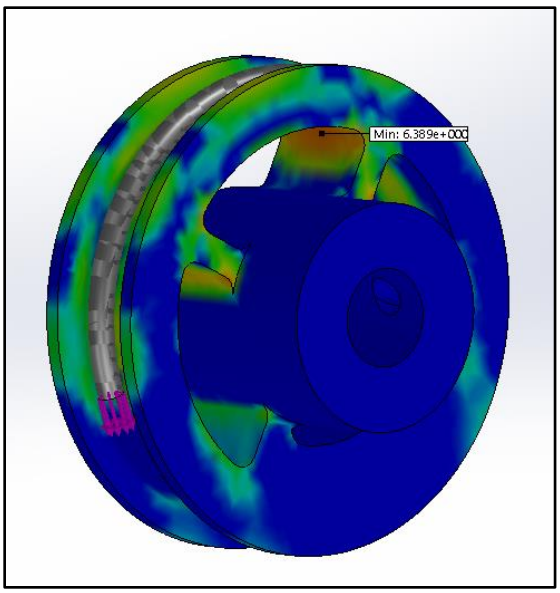

Figure 15: FEA of the motor pulley. This design has a factor of safety of 6.4.

Motor Bracket The motor bracket, Figure 16, was a mounting point for the motor, the upper control plate and the bottom control plate.

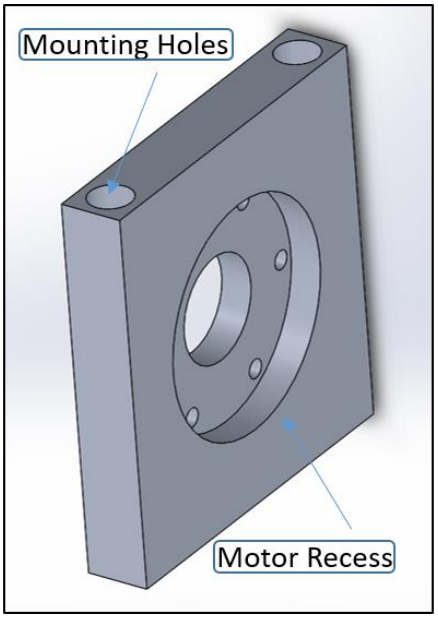

Figure 16: Motor Bracket. Attachment point for both the motor and the control plate.

The minimum mass of the motor bracket is limited by the fasteners used. M5x0.6 fasteners were used to secure the motor bracket, limiting the minimum thickness to 6mm. Because of this the final factor of safety is 52 with a mass of 13.3 g.

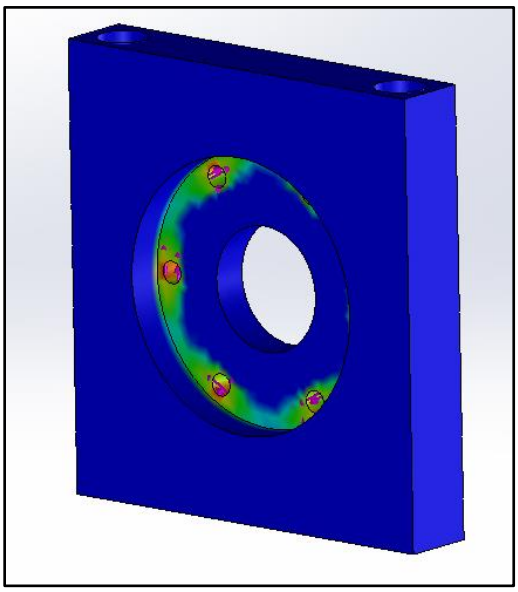

Figure 17: FEA results for the Motor Bracket. Due to dimensional constraints the factor of safety is 52.

Motor Cable Block The Motor Cable Block, Figure 18, served as the proximal end of the Bowden cable outer housing and a mounting point for the control plates. The Bowden cable outer housing needed a rigid location where actuating forces could be applied. The Motor Cable Block had offset holes needed to accommodate the Bowden cable. As the inner wire is wound around the motor pulley it was offset by a distance approximately equal to two times its diameter. These offsets allow for the wire to pass through without rubbing along the sides.

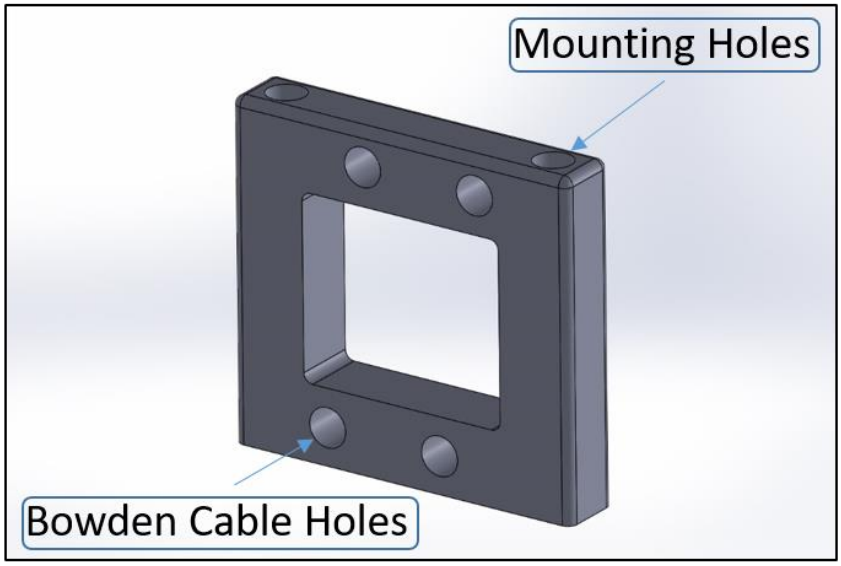

Figure 18: The Motor Cable Block serves as both the proximal end of the Bowden Cable housing and a mounting point for the two control plates.

The minimum size of the block was limited by the M5x0.8 screws used to attach to both the control plates. The height was limited by the diameter of the motor pulley such that the Bowden cable wire would pass straight into the holes without rubbing against the sides. The width was similarly limited by the motor pulley and fastener locations. The final factor of safety is 8.7 with a mass of 14.5 g.

The current design includes the capacity to accommodate two sets of Bowden cables. Future work involving this exoskeleton includes actuating both knee and ankle joints. This requires a total of four holes for two sets of Bowden cables.

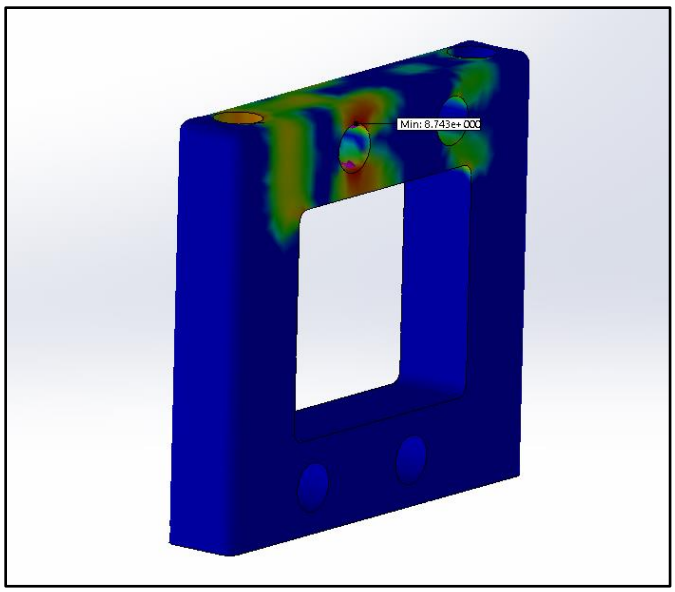

Figure 19: FEA for the Motor Cable Block. The factor of safety is 8.7.

Joint Cable Block The Joint Cable Block's only function is as the distal end of the Bowden cable housing. The design features two angled holes and two mounting holes. The barrel adjuster holes are angled tangent to the ankle pulley. The proximal end of the barrel adjuster holes have a bossed surface for the Bowden cable to seat firmly against.

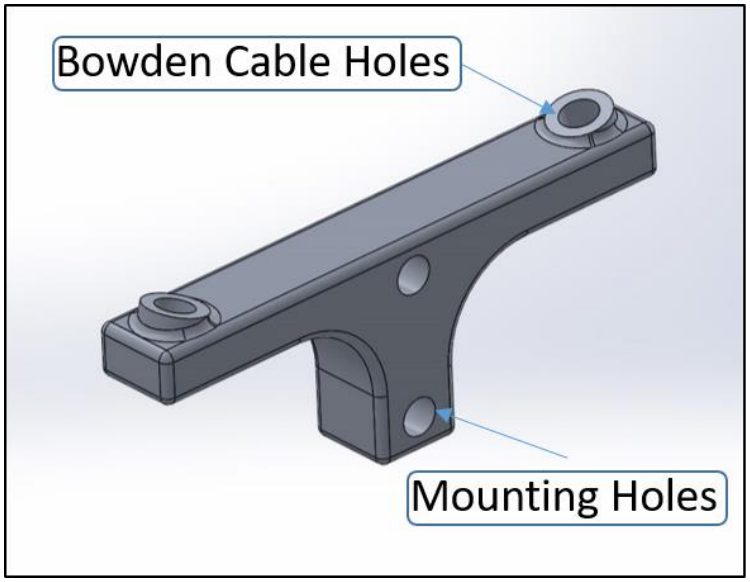

Figure 20: The Joint Cable Block is the distal end of the Bowden cable housing. The angled holes on the top of the block allow the cable to stay tangent to the ankle pulley, reducing friction in the transmission.

The minimum mass of the Joint Cable Block was limited by the required hole sizes. Barrel adjuster threads are M5x0.6 and a M5 nut was used which means that the minimum thickness of the Joint Cable Block was approximately 10 mm. This allows the nut to turn freely without interacting with anything adjacent. The factor of safety of the final design, Figure 21, is 3.8 with a mass of 15.33 g.

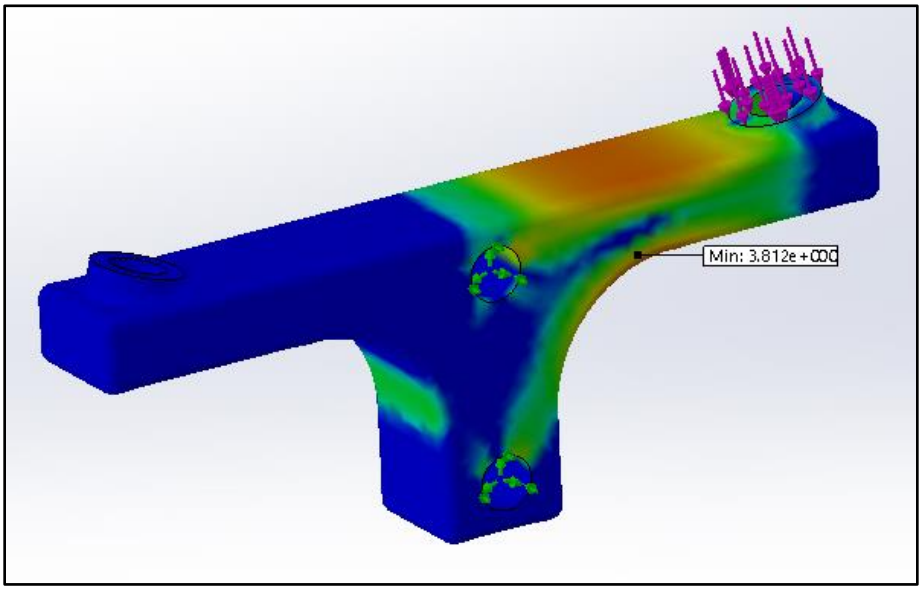

Figure 21: The Joint Cable Block has a high factor of 3.8.

V. Electronics and Controls

A. PCB Design

A custom PCB was designed to meet our specific computational and sensor needs. To keep the cost and complexity of the system low, off-the-shelf components were selected whenever possible. Our PCB design used an Escon Servocontroller, a Teensy 3.2 microcontroller, a Bluetooth module, and connections for two sensors and one Maxon motor. The electronics were powered by a 22.2V Lithium Polymer battery. The Maxon motor was controlled using an Escon module 50/5 servocontroller (Maxon Precision Motors, model number: 438725). The Teensy 3.2 microcontroller was used to control the entire system. The custom PCB is shown in Figure 22.

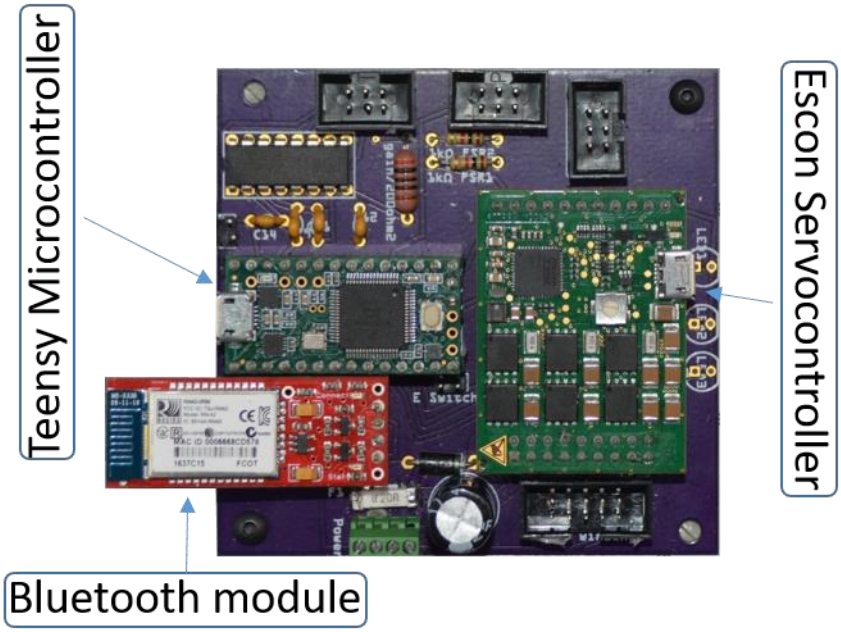

Figure 22: Custom PCB for the ankle Exoskeleton. This PCB has connections for the Teensy microcontroller, Bluetooth module, Escon servocontroller, one motor, and two FSRs.

The Teensy 3.2 was selected for simplicity, small footprint, and processing capability. The Teensy 3.2 can interface with the Arduino Integrated Development Environment (IDE), a popular open-source system that has a large support base with user-made libraries. The Teensy module, shown in Figure 23, is physically smaller than most microcontrollers yet retains sufficient computing power and I/O connections to meet the needs of our system. The main downside of the Teensy compared to other options is that the Teensy lacks built-in peripherals and connection headers.

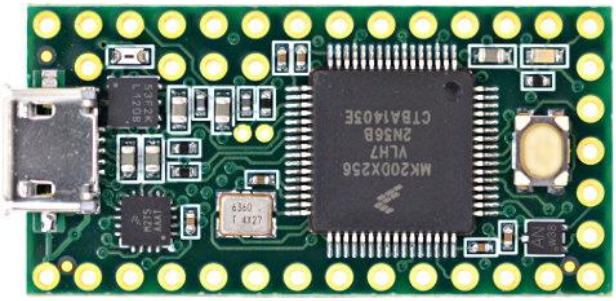

Figure 23: The Teensy 3.2 is an Arduino-based microcontroller with the necessary I/O connections and computing power to operate one joint.

The Escon 50/5 servocontroller provides current control and signal processing for brushless DC motors. Additionally, the controller has the added advantage of providing voltage regulation to other components, including the Teensy microcontroller.

The system was powered by a 22.2V Lithium Polymer (Li-Po) battery. We needed a battery that could reliably power the two PCBs, and the two motors, needed for our exoskeleton. Each motor could possibly draw up to 10 amps of current. Li-Po batteries can easily maintain a constant discharge rate over 20A. Additionally, they have one of the best energy densities among modern batteries. We purchased an E-flite 6S battery. Rated at 22.2V with 910 mAh of capacity, this battery can sustain a constant discharge of 27A. The battery had a mass of 140g.

B. Sensors and Controls

We implemented a custom real-time control scheme. Operation of the system was defined using a two-state Finite State Machine (FSM). A proportional gain control loop was used to control motor torque. Only two sensors per leg were required.

The gait cycle is highly compatible with a FSM. A FSM is a hierarchical control scheme that breaks down the system's functions into a finite number of tasks. The system will transition from one task to another when certain conditions are met. The FSM is very structured and works best when system goals are easily definable and do not need to run concurrently. The gait cycle fits this model well, as you cannot be in both stance phase and swing phase simultaneously. Our FSM defined two states; Assist On and Assist Off. Assistive torque was only applied during the Assist On state. States were triggered using one force sensitive resistor (FSR) under the ball of each foot. During the gait cycle there is an increase in ground reaction forces when the foot is plantarflexing, or pushing against the ground to propel the body forward. Timing of motor torque was determined based on whether the FSR signal was greater than a set threshold value. The threshold was set for each individual as a percentage of the FSR signal read during normal walking.

A torque sensor (Transducer Techniques, model number: TRT-500) closed the loop for ankle torque control. Placed after the transmission system, the torque sensor measured actual ankle torque. We could not use the current-torque relationship of DC motors to estimate torque because of frictional losses in the transmission system. Even with the losses quantified it would not be possible to satisfactorily control the ankle at very low torques.

We controlled motor output using a Proportional, Integral, Derivative (PID) control scheme, which is one of the most ubiquitous control schemes available. PID control measures the difference, or error, between the desired value of a parameter and the actual value. The greater the error, the longer the error exists, or the greater the change in error, the greater the output from the PID. PID has three gains that are tuned for each system, one for P, I, and D. By adjusting these gains it is possible to have a quick and stable response.

For our application, only Proportional feedback was used to control the motor output. We found that the I and D gains did not improve system performance. This is likely due to the dynamics of both the human body and our exoskeleton. A P gain of 300 was found to be satisfactory for the operation of our ankle exoskeleton.

Signal filtering reduced noise and improved system stability. All sensors are susceptible to electromechanical noise. If the feedback control is highly responsive, which is typically desired, then it may be susceptible to noise. To improve control stability it is common to filter raw sensor data and feed the filtered data to the controller. The downside of filtering is that it causes a delay between what is measured and what is reported. System stability can be improved by balancing the tradeoff of delay and filtering. We filtered our data using a 3-sample running average.

Torque profiles were controlled to match the smooth curves of natural ankle torque. Transitioning between Assist On and Assist Off states, without any adjustment to torque setpoint, would result in a square wave torque profile. This sudden load may be hard on the user. To more closely align with natural torque

profiles we used a sigmoid function to smooth changes in the torque setpoint. Not only did this result in more natural assistance but it also improved control stability by reducing the instantaneous error between measured and desired torque.

The motor controller operated at 1000 Hz, while data were recorded at 100 Hz. We recorded torque setpoint, measured torque, FSM state values, and FSR voltages for both legs.

C. User Interface

We made a graphical user interface (GUI) in Matlab that connected to the exoskeleton over Bluetooth. Our GUI displayed and recorded data from the exoskeleton and could also change the operating parameters of the exoskeleton between tests. The parameters we could change include PID gains, Assist On torque setpoint, and the shape of the torque smoothing function. Figure 24 shows the GUI that was used.

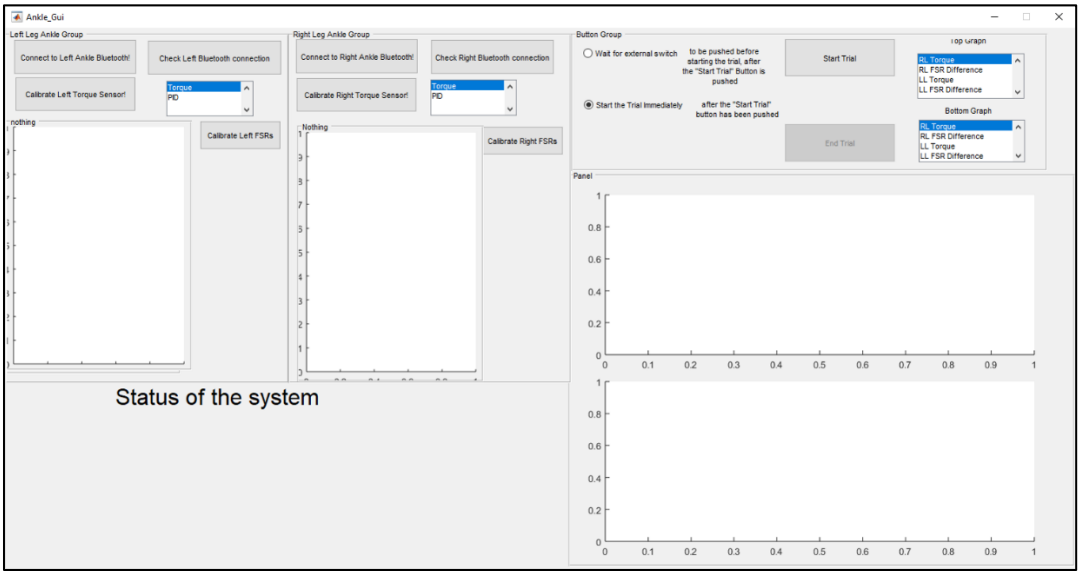

Figure 24: The Matlab GUI. The right side of the GUI plots recorded data. The left side handles Bluetooth management and user inputs.

D. Safety

To ensure the safe use of this device we implemented five safety measures. First, the microcontroller was coded to limit motor current. Second, the servocontroller parameters were set to limit motor current. Third, a fuse was installed to prevent the motors from overdrawing current. Fourth, the motors were disengaged if the torque sensor reading exceeded a threshold value. Fifth, an emergency shutoff switch was placed such that the motors could be immediately disengaged. With these five precautions we are confident in the safe operation of our system.

VI. EXOSKELETON ANALYSIS METHOD

We completed a pilot study to evaluate the ability of our design to reduce the energy cost of walking in individuals with CP. Three participants completed 6 visits at NAU's Human Performance Lab where they practiced walking with powered ankle assistance from the exoskeleton. We quantified the energy cost of walking based on the volume of consumed O_2 ($\dot{V}O_2$) and volume of produced CO_2 ($\dot{V}CO_2$) according to [25][32]. We recorded torque profiles to show the torque used to reach our outcomes. Metabolic data was also used to quantify the accuracy of our metabolic estimate using effective mass.

A. Instrumentation

A Cosmed portable metabolic testing device (K5) was used to measure oxygen consumption ($\dot{V}O_2$) and carbon dioxide production ($\dot{V}CO_2$). The measurements were used to estimate metabolic cost based on [25][32]. The K5 mobile metabolic system is a standalone, battery-powered, self-contained device that can be worn by the user allowing a freedom of movement and activity. For our testing, the K5 was suspended in front of the participant to remove the mass of the K5 from metabolic consideration. Figure 25 shows a participant wearing the exoskeleton and metabolic system.

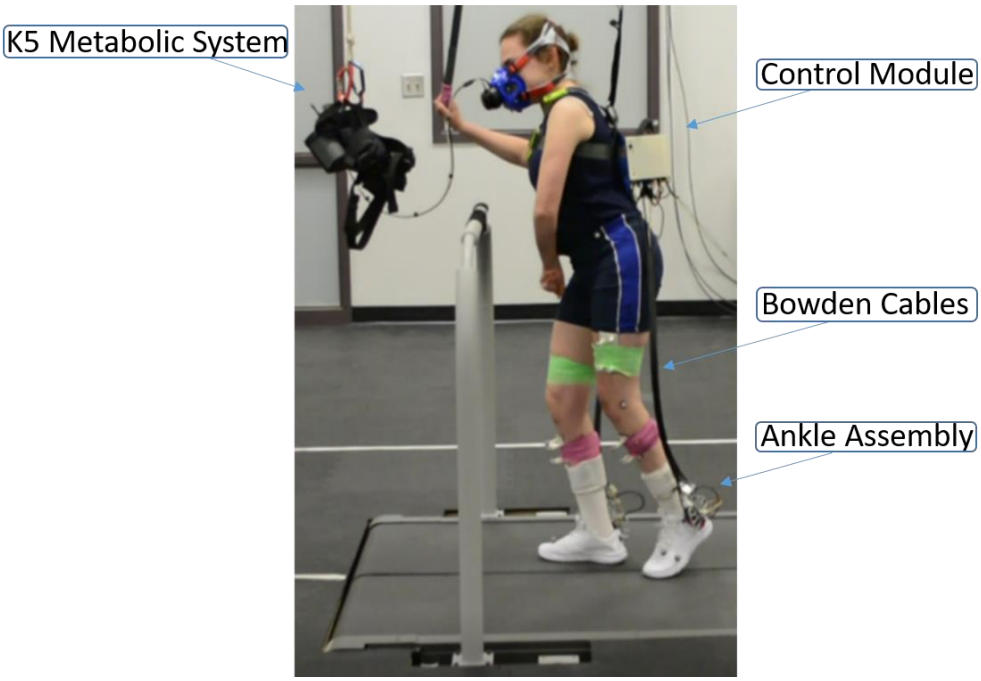

Figure 25: A study participant wearing the ankle exoskeleton and K5 metabolic mask.

B. Pilot Study

Each individual participated in a 6-visit study. The first visit consisted of a physical evaluation and orthotic measurements performed by a registered physical therapist assisting with the study. The second visit was a fitting of the custom orthotics for the exoskeleton. The third and fourth visits were training periods with the exoskeleton. The fifth and sixth visits were data collection visits where each participant walked on a treadmill under our three test conditions while wearing a metabolic mask. Participant data is available in Table 7.

Table 7: Summary of participant data. Participants vary in size from 16 to 45.5 kg. This covers the entire expected size range for our participants. The mass of the device is given as a percentage of the participant's body mass.

ID	Mass (kg)	Device Mass (%)	Height (m)	Age	Severity
P1	16	12.5%	0.98	5	Mild
P2	26.8	7.5%	1.27	7	Mild
P3	45.5	4.4%	1.47	22	Moderate

Data were collected under three walking conditions: baseline, zero-torque, and power assist. For the baseline condition, each participant walked using their preferred footwear and/or AFOs. For the zero-torque condition, each participant walked with the exoskeleton while the system was attempting to maintain a zero-torque reading at the ankle. For the power assist condition, each participant walked with exoskeleton assistance.

The baseline and zero conditions should be similar except for the additional mass of the exoskeleton. The intent of the zero-torque condition was to remove all effects of wearing the exoskeleton except for added mass. When the exoskeleton is unpowered the wearer bears the additional weight of the system and the friction of the cables and inertia of the motors. However, during zero-torque the system attempts to compensate for both friction and motor inertia. The result is that the user may move freely, need only to support the added mass of the exoskeleton.

The power assist condition applied user-specific torque. During visits three and four, we selected the assistance best suited for each participant. Initial values were chosen as an approximation based on their mass. We then adjusted the torque level during an assisted-walking period until the participant was comfortable with the assistance.

The participants walked at a self-selected speed under the three different conditions for five minutes. Metabolic data was averaged over the final minute of the 5-minute walking trial, which allowed 4 minutes for the participant to reach steady-state.

VII. Results and Discussion

A. Metabolic Rate (Assisted vs. unassisted vs. typical)

Ankle plantarflexion assistance reduced the metabolic cost of walking. Figure 26 compares the metabolic rate of the three participants between baseline, zero-torque, and powered walking conditions. For each participant there was a metabolic rate decrease between the zero-torque and assisted conditions.

Two of the three participants also showed a metabolic rate decrease between the baseline and assisted conditions.

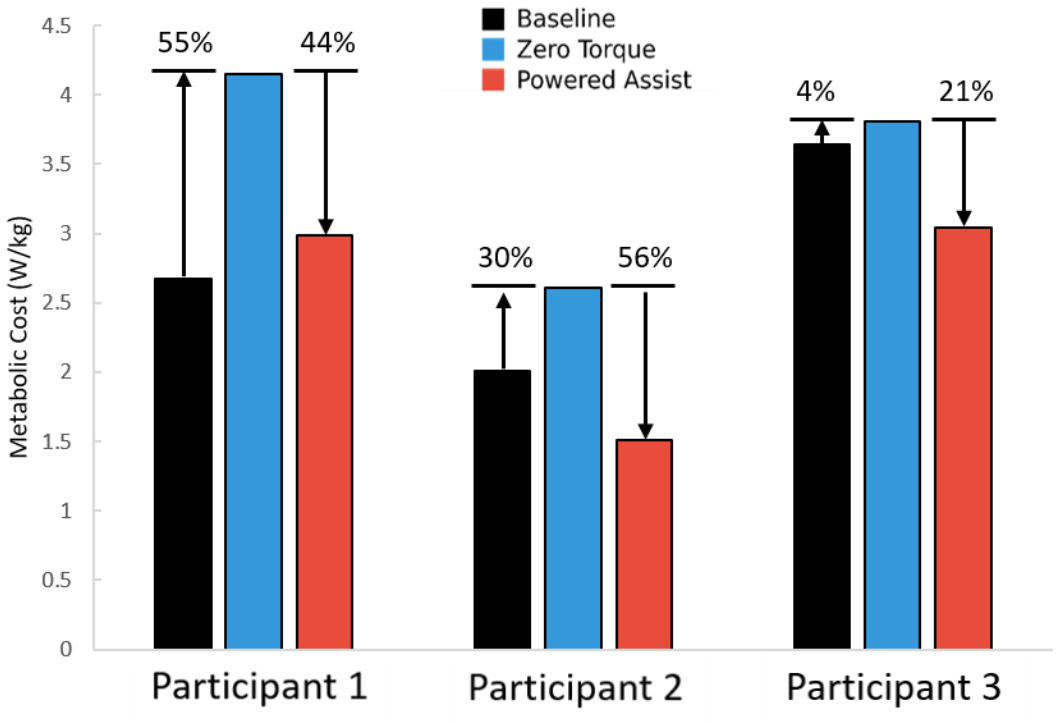

Figure 26: Measured metabolic rate of the three participants. All participants showed a decrease in net metabolic cost between the zero-torque and assisted conditions. Only P1, the smallest participant, did not show a decrease between baseline and assisted conditions. The largest reduction below baseline was for P3 at 26%.

P1 showed an increase in metabolic rate of 11% between baseline and assisted walking conditions. This may be related to the relative mass of the system to the wearer. P1 was our lightest participant at 16 kg, meaning our system was 13% of their total mass. P2 and P3 were much larger with the system being only 4.4% and 7.5% of their body mass, respectively. P1 also showed the largest increase in metabolic rate between baseline and zero-torque at 55% compared to P2 at 4% and P3 at 30%. This means that the work required for P1 to walk with the exoskeleton was much greater than other participants.

It is reasonable to assume that smaller users will see a more limited reduction in metabolic cost. Our system can reduce biological ankle work but the mass of the device would increase knee and hip work. If the increase in metabolic rate from knee and hip work is greater than the decrease due to ankle assistance then we would expect to observe a net increase in metabolic rate.

B. *Torque profile (Assisted vs. unassisted vs. typical)*

A properly working assistive device will apply torque that is repeatable, reliable, and large enough to reduce the net metabolic rate. Having repeatable and reliable torque allows the wearer to adapt to the assistance. Figure 27 shows that the desired torque was met in both the assisted and zero-torque conditions.

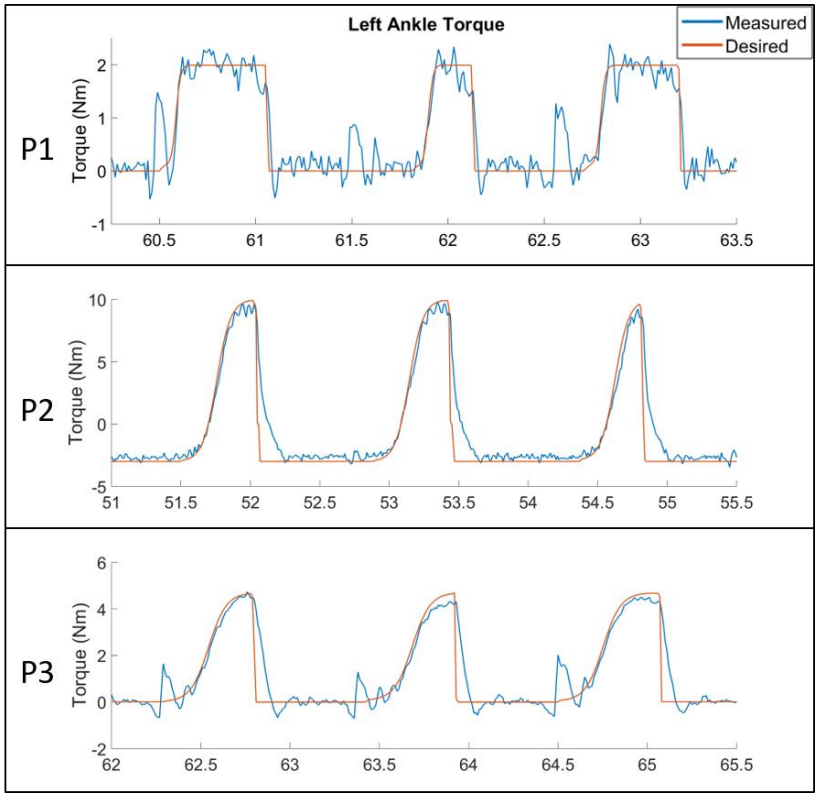

Figure 27: Sample torque profiles for the three participants. Blue represent measured torque and red represents the torque setpoint. For all three participants our controller was sufficient to reach the desired torque levels.

C. *Effective Mass metabolic prediction vs. measured metabolic rate*

In section IV.E, we predicted the metabolic effect of adding additional mass to the wearer using the Effective Mass Equation (1). Figure 27 summarizes the predicted increase of net metabolic rate during zero-torque and the actual measured values.

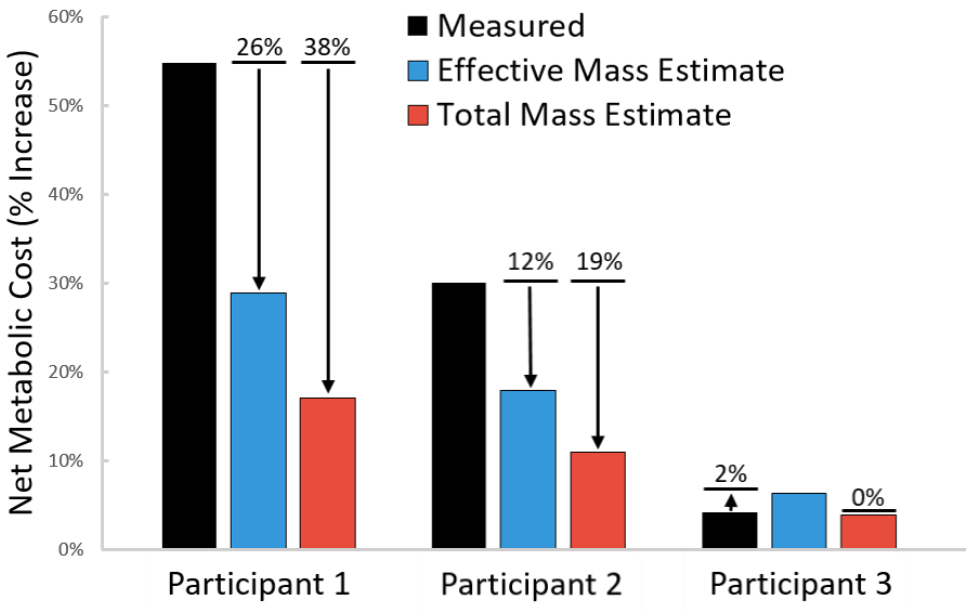

Figure 28: Comparison of metabolic rate estimations using Effective Mass and total mass. Metabolic rate was measured during the zero-torque walking condition. In general, Effective Mass was a better predictor of metabolic rate than total mass. However, the percent error of Effective Mass is much higher than desired.

Effective Mass appears to be a more accurate estimator of net metabolic increase than total mass. The average error of net metabolic rate estimated using total mass was over two times greater than when it was estimated using our Effective Mass Equation (1). This indicates that appropriately accounting for both mass and location may lead to more accurate estimates of net metabolic rate increase. However, effective mass still had an error of 58%. We believe that this error is primarily related to the strength of the studies we used to derive the Effective Mass equation. Replicating the work in [35] and [37] using populations with CP may lead to a more accurate relationship. This is further supported by the apparent trend in decreasing error as participant mass increases from the smallest on the left to the largest on the right.

It is interesting to note that for Participant 3 that the total mass percent error is smaller than the Effective Mass percent error. It is possible that the equation used [35] is the primary source of this discrepancy. As user mass approaches the average mass in [35] the error approached zero.

VIII. CONCLUSION

We have presented an assistive ankle exoskeleton that is capable of reducing the metabolic cost of walking in individuals with CP. The designed and tested battery-powered system weighs 2 kg and can apply up to 12 Nm of torque. Our data suggests that it can reduce the net metabolic rate of walking in children and young adults with CP.

While not all participants showed a decrease in metabolic rate below their baseline, all showed a reduction when compared to the zero-torque condition. The only participant that did not have a decrease in metabolic rate was much smaller than the other participants. This may be due to added loads to knees and hips that are not assisted by the exoskeleton.

Our effective mass equation was a more accurate indicator of net metabolic increase than total mass but leaves much room for improvement. The average estimated error using effective mass was 58% while the total mass estimate was 133%. Our equation was derived using previously published data from a non-CP population walking under different conditions. The effective mass equation should be rederived using a data set from CP populations.

A. Limitations

The size of the study limits confidence in our findings. With three participants that span a wide range of ages, sizes, masses, and motor function capability our results demonstrate a strong potential for clinically-relevant improvement in the energy cost of walking in this heterogeneous population. However, additional testing in more participants is needed to improve the generalizability of our findings.

The derivation of the current effective mass equation is known to have four important limitations. First, in [37] a group of five healthy men participated in the study. Data collected from that population may not necessarily correlate to impaired populations. Second, the sample size was small enough that additional

studies would improve confidence in the equation. The third limitation is that the base metabolic rate for all participants was estimated at $2.36\frac{W}{kg}$ but that rate varies between individuals. What is not reported in [37] is whether adding mass has equal effects on all participants. Finally, masses were only placed at the COM location of each lower-extremity segment. Additional locations would offer insight into how gait biomechanics interact with moments of inertia. Despite these limitations it is assumed that the data has enough relevance to be a guide for design decisions.

Similar to the limitations of the effective mass equation, the mass-to-metabolic relationship reported in [35] has two limitations. The sample size was limited to ten healthy participants, meaning that the data may not be applicable to our population. Furthermore, the data was only recorded at 1.25 m/s walking speed. We do not currently know the relationship between speed, mass, and metabolic rate. With all the limitations of these two studies we expect to have errors in our calculations but they should still yield valuable data.

B. Future Work

This thesis presents an early exoskeleton prototype, the first for the Biomechatronics Lab at Northern Arizona University. Future development may show improvements in mass optimization, assistance timing and magnitude, comfort, and reliability.

Mechanical Design Aluminum 6061-T6 may be unnecessarily strong for some components. The current design uses aluminum for nearly every component. While relatively inexpensive and machinable, not all components require the strength of aluminum. It may be valuable to investigate alternative materials. Some components, such as the Motor Cable Block, have very large factors of safety. Optimizing material selection could lead to weight savings, fabrication time reduction, and significant cost savings.

The current design follows a “one-size-fits-all” policy. While most of the orthotics are custom-fabricated for each participant there are several components that may benefit from custom manufacturing

based on user size. The ankle pulley is engineered to be able to withstand a maximum load of 270 N (12 Nm of torque) with a factor of safety of 1.8. While necessary for larger participants who need large torques, smaller participants are using only a third of that. Replacing the 3:1 gearing ratio with a 1:1 would decrease weight, shift the max efficiency torque from 9.61 Nm to 3.20 Nm, and reduce bulk. Lower loads may also enable the use of thinner components.

Lowering the effective mass will improve the impact of the system on biomechanics. The current system has a mass of 2 kg and an effective mass of 3.11kg. It may still be possible to reduce the effective mass. Some components, such as the Motor Bracket and Motor Cable Block, were limited by the size of the fasteners used. Using smaller fasteners would allow for thinner components. Other avenues include optimizing the mechanical design by using other materials or increasing the size and number of weight-saving holes.

The minimum size of some components was limited by fastener selection. The Motor Cable Block is one example of a component that could be made smaller if a smaller fastener was used. M5x0.8 screws attached the Motor Cable Block to both the control and motor plates. If it is possible to change the fastener to an M3x0.5 then the thickness of the component could possibly be reduced by over 30%. While the Motor Cable Block is a very small portion of the overall mass, and it exists above the waist, all mass savings can be valuable.

Improving the conformity of the exoskeleton to the individual may improve both the perceived and measured effect. It was observed that Participant 2 would often hold onto the Bowden cables. He said that he did not like the cables waving back and forth. It could be possible to constrain the cables to follow a more stable path. Possible difficulties would be an increase in friction as the cable bends due to an increase in path length. This may necessitate an auto tensioning system to compensate for path length discrepancies.

Battery Life Frictional losses between motor and ankle may be causing a significant reduction in battery life. One of the major sources of friction is in the Bowden cable system. A possible way to reduce

friction is to use a shift cable instead of brake cable. Shift cables are thinner, lighter, and do not change tension when bent. Two main issues may exist with this change. First, because the cables are thinner then are more likely to fail. We do not know if shift cables can withstand the loads of the motor. Second, the housing is more likely to fail. Brake cable housing is made of a tightly wound cable but shift cable housing is made of several thin wires running the length of the cable. This design allows the inner wire to maintain a steady tension regardless of the cable bending. However, the housing is more likely to buckle. We do not know if the housing can withstand the forces the motor will apply.

The motor's maximum efficiency point exists at a certain torque and speed. We do not maintain that set point for long. Research has been done in using a motor to store potential energy in a spring and then using the spring to apply the assistive torque. If the motor, gear ratio, and spring were properly specified it could be possible to run the motor at maximum efficiency for long periods and still accomplish the same work as the current system. This may significantly improve efficiency.

Controls The simplicity of the controller may have inhibited the exoskeleton's effectiveness. A more advanced FSM with more states and better torque control to match biological ankle torque profiles may improve the effect of the system.

Onboard optimization routines may improve system performance. Controller parameters are adjusted for each individual by tuning it for a single speed and walking condition. In typical walking, ankle torque and angular velocity change as a function of walking speed. Understanding the relationship between speed and torque would permit the development of a controller that would continually adjust assistive torque to give the best result.

Study Our experimental procedure can help validate the effectiveness of the exoskeleton and provide greater insight into future improvement. The study presented here had only three participants were very different from each other. Because of their differences it is hard to generalize our findings. Future studies with more participants may close the gap in our research.

IX. REFERENCES

[1] S and E. tanley, Fiona J and Blair, Eve and Alberman, *Cerebral palsies: epidemiology and causal pathways*, vol. 151. Cambridge University Press, 2000.

[2] E. Himpens, C. Van Den Broeck, A. Oostra, P. Calders, and P. Vanhaesebrouck, "Prevalence, type, distribution, and severity of cerebral palsy in relation to gestational age: A meta-analytic review," *Developmental Medicine and Child Neurology*. 2008.

[3] E. Odding, M. E. Roebroeck, and H. J. Stam, "The epidemiology of cerebral palsy: Incidence, impairments and risk factors," *Disabil. Rehabil.*, vol. 28, no. 4, pp. 183–191, Jan. 2006.

[4] P. Rosenbaum *et al.*, "A report: The definition and classification of cerebral palsy April 2006," *Dev. Med. Child Neurol.*, 2007.

[5] T. M. O'Shea, "Diagnosis, treatment, and prevention of cerebral palsy," *Clin. Obstet. Gynecol.*, 2008.

[6] H. Kerr Graham and P. Selber, "Musculoskeletal aspects of cerebral palsy," *J. Bone Jt. Surg.*, 2003.

[7] D. C. Johnson, D. L. Damiano, and M. F. Abel, "The evolution of gait in childhood and adolescent cerebral palsy," *J. Pediatr. Orthop.*, 1997.

[8] K. F. Bjornson, B. Belza, D. Kartin, R. Logsdon, and J. F. McLaughlin, "Ambulatory Physical Activity Performance in Youth With Cerebral Palsy and Youth Who Are Developing Typically," *Phys. Ther.*, 2007.

[9] C. G. Gajdosik and N. Cicirello, "Secondary Conditions of the Musculoskeletal System in Adolescents and Adults with Cerebral Palsy," *Phys. Occup. Ther. Pediatr.*, vol. 21, no. 4, pp. 49–68, Jan. 2002.

[10] K. M. Steele, A. Seth, J. L. Hicks, M. H. Schwartz, and S. L. Delp, "Muscle contributions to vertical and fore-aft accelerations are altered in subjects with crouch gait," *Gait Posture*, vol. 38, no. 1, pp. 86–91, 2013.

[11] T. E. Johnston, S. E. Moore, L. T. Quinn, and B. T. Smith, "Energy cost of walking in children with cerebral palsy: relation to the Gross Motor Function Classification System.," *Dev. Med. Child Neurol.*, vol. 46, no. 1, pp. 34–38, 2004.

[12] J. G. Nutt, C. D. Marsden, and P. D. Thompson, "Human walking and higher-level gait disorders, particularly in the elderly," *Neurology*, vol. 43, no. 2, p. 268 LP-268, Feb. 1993.

[13] J. M. Donelan, D. W. Shipman, R. Kram, and A. D. Kuo, "Mechanical and metabolic requirements for active lateral stabilization in human walking," *J. Biomech.*, vol. 37, no. 6, pp. 827–835, 2004.

[14] I. novak *et al.*, "A systematic review of interventions for children with cerebral palsy: State of the evidence," *Developmental Medicine and Child Neurology*. 2013.

[15] S. Khamis, R. Martikaro, S. Wientroub, Y. Hemo, and S. Hayek, "A functional electrical stimulation system improves knee control in crouch gait," *J. Child. Orthop.*, 2015.

[16] S. Gusso *et al.*, "Effects of whole-body vibration training on physical function, bone and muscle mass in adolescents and young adults with cerebral palsy," *Sci. Rep.*, 2016.

[17] I. S. Corry, A. P. Cosgrove, C. M. Duffy, T. C. Taylor, and H. K. Graham, "Botulinum toxin A in

hamstring spasticity," *Gait Posture*, 1999.

[18] S. A. Galey, Z. F. Lerner, T. C. Bulea, S. Zimbler, and D. L. Damiano, "Effectiveness of surgical and non-surgical management of crouch gait in cerebral palsy: A systematic review," *Gait and Posture*. 2017.

[19] S. K. Banala, S. H. Kim, S. K. Agrawal, and J. P. Scholz, "Robot assisted gait training with active leg exoskeleton (ALEX)," in *Proceedings of the 2nd Biennial IEEE/RAS-EMBS International Conference on Biomedical Robotics and Biomechatronics, BioRob 2008*, 2008.

[20] S. Lefmann, R. Russo, and S. Hillier, "The effectiveness of robotic-assisted gait training for paediatric gait disorders: Systematic review," *Journal of NeuroEngineering and Rehabilitation*. 2017.

[21] A. J. Hilderley, D. Fehlings, G. W. Lee, and F. V. Wright, "Comparison of a robotic-assisted gait training program with a program of functional gait training for children with cerebral palsy: design and methods of a two group randomized controlled cross-over trial," *Springerplus*, vol. 5, 2016.

[22] I. Schwartz and Z. Meiner, "Robotic-Assisted Gait Training in Neurological Patients: Who May Benefit?," *Ann. Biomed. Eng.*, vol. 43, no. 5, pp. 1260–1269, May 2015.

[23] Z. Lerner, D. Damiano, H.-S. Park, A. Gravunder, and T. Bulea, "A Robotic Exoskeleton for Treatment of Crouch Gait in Children with Cerebral Palsy: Design and Initial Application," *IEEE Trans. Neural Syst. Rehabil. Eng.*, 2016.

[24] Z. F. Lerner, D. L. Damiano, and T. C. Bulea, "A robotic exoskeleton to treat crouch gait from cerebral palsy: Initial kinematic and neuromuscular evaluation," in *Proceedings of the Annual International Conference of the IEEE Engineering in Medicine and Biology Society, EMBS*, 2016.

[25] M. Matsuda, Y. Mataki, and H. Mutsuzaki, "Immediate effects of a single session of robot-assisted gait training using Hybrid Assistive Limb (HAL) for cerebral palsy," pp. 207–212, 2018.

[26] C. Report *et al.*, "Use of Hybrid Assistive Limb - for a postoperative patient with cerebral palsy : a case report," *BMC Res. Notes*, pp. 1–7, 2018.

[27] J. M. Ryan, E. E. Cassidy, S. G. Noorduyn, and N. E. O'Connell, "Exercise interventions for cerebral palsy," *Cochrane Database of Systematic Reviews*. 2017.

[28] D. J. Farris and G. S. Sawicki, "The mechanics and energetics of human walking and running: a joint level perspective," *J. R. Soc. Interface*, 2012.

[29] M. Q. Liu, F. C. Anderson, M. H. Schwartz, and S. L. Delp, "Muscle contributions to support and progression over a range of walking speeds," *J. Biomech.*, vol. 41, no. 15, pp. 3243–3252, 2008.

[30] D. Maltais, O. Bar-Or, V. Galea, and M. Pierrynowski, "Use of orthoses lowers the O(2) cost of walking in children with spastic cerebral palsy.," *Med. Sci. Sports Exerc.*, vol. 33, no. 2, pp. 320–325, 2001.

[31] M. A. Brehm, J. Harlaar, and M. Schwartz, "Effect of ankle-foot orthoses on walking efficiency and gait in children with cerebral palsy," *J. Rehabil. Med.*, 2008.

[32] J. J. Eng and D. A. Winter, "Kinetic analysis of the lower limbs during walking: What information can be gained from a three-dimensional model?," *J. Biomech.*, vol. 28, no. 6, pp. 753–758, 1995.

[33] Z. F. Lerner, D. L. Damiano, and T. C. Bulea, “The effects of exoskeleton assisted knee extension on lower-extremity gait kinematics, kinetics, and muscle activity in children with cerebral palsy,” *Sci. Rep.*, vol. 7, no. 1, pp. 1–12, 2017.

[34] J. S. Gottschall, “Energy cost and muscular activity required for leg swing during walking,” *J. Appl. Physiol.*, vol. 99, no. 1, pp. 23–30, 2005.

[35] A. Grabowski, “Independent metabolic costs of supporting body weight and accelerating body mass during walking,” *J. Appl. Physiol.*, vol. 98, no. 2, pp. 579–583, 2004.

[36] C. L. Brockett and G. J. Chapman, “Biomechanics of the ankle,” *Orthop. Trauma*, vol. 30, no. 3, pp. 232–238, 2016.

[37] R. C. Browning, J. R. Modica, R. Kram, and A. Goswami, “The effects of adding mass to the legs on the energetics and biomechanics of walking,” *Med. Sci. Sports Exerc.*, 2007.

[38] A. M. Dollar and H. Herr, “Lower extremity exoskeletons and active orthoses: Challenges and state-of-the-art,” *IEEE Trans. Robot.*, vol. 24, no. 1, pp. 144–158, Feb. 2008.

[39] R. Bogue, “Exoskeletons and robotic prosthetics: a review of recent developments,” *Ind. Robot An Int. J.*, vol. 36, no. 5, pp. 421–427, 2009.

[40] K. A. Shorter, G. F. Kogler, E. Loth, W. K. Durfee, and E. T. Hsiao-Wecksler, “A portable powered ankle-foot orthosis for rehabilitation,” *J. Rehabil. Res. Dev.*, vol. 48, no. 4, p. 459, 2011.

[41] T. M. Griffin, T. J. Roberts, and R. Kram, “Metabolic cost of generating muscular force in human walking: insights from load-carrying and speed experiments,” *J. Appl. Physiol.*, 2003.

X. Appendix

A. Bowden Cables

The Bowden cable operates on equal and opposite reactions between housing and cable. The forces and operation of the Bowden cable are illustrated in Figure 29. A straight cable between two levers attached to the same rigid ground. Applying a force to one lever will actuate both equally and an opposing force is transferred to the ground. However, Bowden cables do not require both points to be rigidly fixed to the same structure.

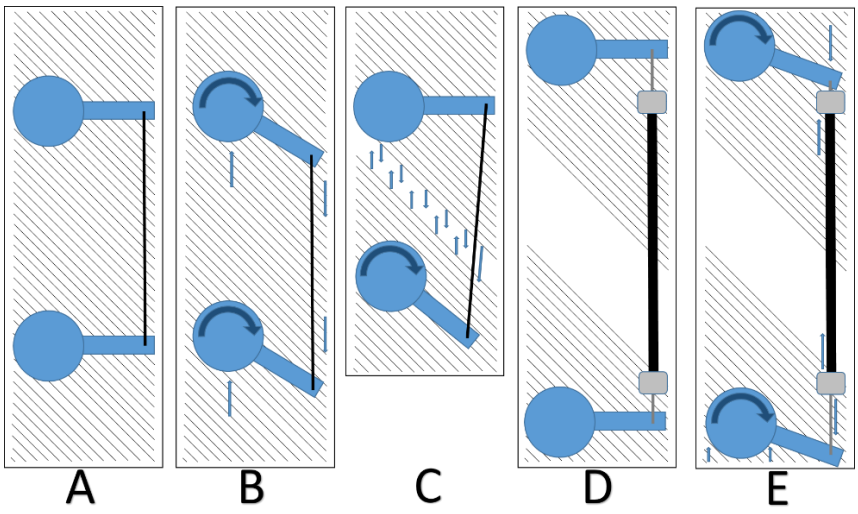

Figure 29: The operation of Bowden cables. (A) Two levers that share a common ground and are connected by a straight wire. (B) Actuating one lever in (A) actuates the opposing lever. (C) Remove the common ground and allow relative motion between the two separate structures. When on lever is rotated the two structures move closer together. (D) An incompressible housing and rigid mounting blocks are added to (C). (E) Actuating one lever will actuate the opposing lever without moving the two structures.

If we replace the single common rigid structure with two separate structures, Figure 29 (C), then the single actuating line loses its function. If the two separate structures are free to move relative to each other then rotating one lever is just as likely to pull the structures together as it is to rotate the other lever.

Bowden cables have the capacity to actuate the levers remotely without moving the separate structures. The primary issue with the previous example is that the opposing load moves the structures together. There needs to be a means of transferring the opposing load to the other structure without binding them together. This is the function that the outer housing serves. In this example, Figure 29 (D) and (E), the housing is firmly fixed between two mounting blocks. When on lever is actuated the wire is pulled. The load is transferred to the ground. However, because the housing is incompressible and the mounting blocks are rigid, the distance between the structures remains fixed. The load is transferred from the ground, to the block, through the housing, to the other block and to the other structure. Additionally, the wire no longer must follow a straight line as a bent housing will still transfer the load. Remote actuation is now possible between two points that do not share the same common ground.

There remain two important points in the operation of Bowden cables. A free length of housing will buckle under compression but not while its inner wire is under tension. This is due to tension increasing when the housing is bent. Recall that the housing is a tightly wound metal coil. When bent, the inner coils push again each other with virtually no compression. Instead, the outer coils separate. This forces the inner wire to follow a path that is longer than the straight path. This increases the wire tension. The wire attempts to release tension by straightening but the housing attempts to release compression by buckling. Because of the balance of forces the Bowden cable does not buckle.

The final important note about Bowden cable operation is relates to controlling cable tension. The greater the tension in a wire, the straighter the path it will follow. By controlling the distance between housing end and wire end, tension can likewise be controlled. A barrel adjuster, shown in Figure 30, is a threaded bolt with a hole through its center and a cup in place of the head. The housing is seated into the cup and the wire is passed through the hole. By threading the barrel adjuster in to the blocks in Figure 29 (D) the distance between housing end and wire end is decreased, which releases wire tension. Conversely, unthreading the barrel adjuster will increase tension.

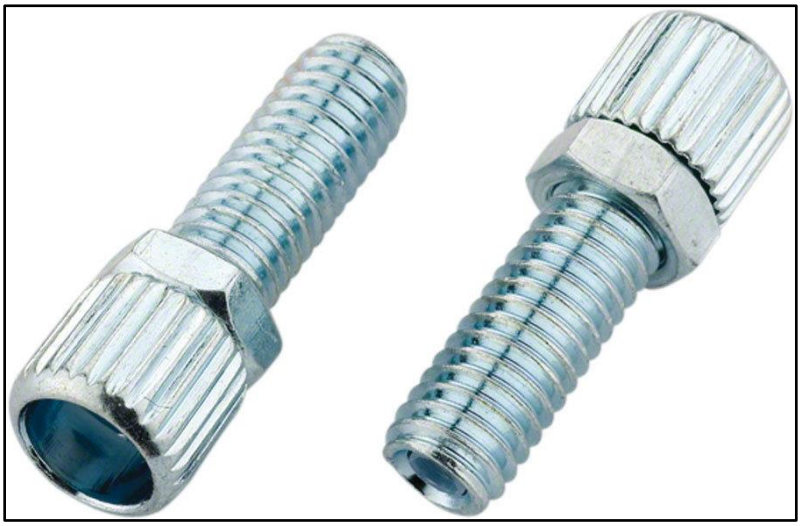

Figure 30: A barrel adjuster allows fine tuning of tension in a Bowden cable by controlling the distance between the end of the housing and the end of the cable.